Universidade do Algarve
Faculdade de Ciências do Mar e do Ambiente

Systematic comparison on the inundation response of AnuGA and COMCOT Tsunami modelling codes applied to the Boca do Rio and Alvor Bay area

Miguel André Gonçalves Fernandes

Mestrado em Oceanografia

Faro
Fevereiro de 2009

Universidade do Algarve
Faculdade de Ciências do Mar e do Ambiente

Systematic comparison on the inundation response of AnuGA and COMCOT Tsunami modelling codes applied to the Boca do Rio and Alvor Bay area

Miguel André Gonçalves Fernandes

Mestrado em Oceanografia

Dissertação orientada por:
Professor Doutor Joaquim Freire Luis (Universidade do Algarve)

Faro
Fevereiro de 2009

Abstract

This work is integrated in the Portuguese efforts to study tsunami hazard and risk on the Algarve coast and to develop emergency plans by the Portuguese Civil Protection. As part of this broader purpose, the objective of this study is to compare the inundation response of tsunami numerical models. Off the models available to this study, we have selected for comparison: model COMCOT based on a finite difference scheme to discretize non-linear shallow water wave equations (NLSWE) and model AnuGA based on the finite volume method for the evaluation of NLSWE.

We started by validating the numerical codes with analytical and laboratory benchmarks proposed at the 2004 Catalina Long Wave Congress. A first test case was performed at Boca do Rio valley where historical and sedimentological data from the 1755 Lisbon tsunami was available. Its purpose was to properly configure the numerical models to the Algarve coast by comparing the modelled results with the historical data. We have found a good agreement with the historical data, even though the *run-in* was underestimated.

A systematic comparison of the inundation response of the numerical models was performed at Alvor Bay. The response was measured by the *run-up* and *run-in* parameters. We have constructed 81 fault models to create the initial conditions for the tsunami codes based on the variation of fault parameters: dip and depth. A good agreement was found in AnuGA and COMCOT propagation modelling. The differences found in the *run-up* and *run-in* parameters seem to be related to the inundation methods. COMCOT has always produced higher inundation parameters than AnuGA. Nevertheless, the results obtained with AnuGA have been more consistent. The maximum inundation on the cases teste have been obtained with proximate source models while COMCOT has revealed a large span of source models able to produce maximum inundation.

Key-words: Run-up; Run-in; tsunami model comparison; AnuGA; COMCOT;

Resumo

O trabalho levado a cabo encontra-se inserido no estudo do risco sísmico e de tsunami no Algarve da Autoridade Nacional de Protecção Civil (ANPC). O objectivo deste trabalho é o de efectuar uma comparação sistemática de modelos numéricos de tsunami baseado nos parâmetros de inundação *run-up* e *run-in*.

Os modelos de tsunami mais utilizados em investigação em Portugal têm sido: o SWAN [25], o TUNAMI-N2 [18], o MOST [41] e o COMCOT [22]. No entanto, o primeiro apenas permite modelar a propagação e apesar de ter sido utilizado durante o trabalho não foi incluído na comparação. O segundo também não foi escolhido, uma vez que apresenta a limitação de apenas ser possível utilizar um nível de resolução espacial, o que não é adequado aos objectivos do trabalho. Infelizmente, o terceiro não esteve á disposição do projecto e por isso não foi utilizado. O quarto tem sido utilizado no âmbito do projecto Europeu TRANSFER e enquadra-se nos objectivos e foi um dos escolhidos. Foram também analisados os modelos CLAWPACK [20] e AnuGA [30]. O primeiro apresentou igualmente problemas ao nível do controlo da resolução espacial e foi por este motivo não incluído. O segundo é um modelo que utiliza uma malha triangular para discretizar a topografia que permite um bom controlo da resolução na zona a estudar, foi por este motivo incluído no trabalho.

O primeiro passo do trabalho foi o de efectuar uma validação dos modelos numéricos. Foram utilizados dois *benchmarks* propostos no Congresso de Ondas-Longas realizado em Catalina, EUA em 2004. Um primeiro *benchmark* permite a validação com uma solução analítica e um segundo *benchmark* permite a validação com dados laboratoriais obtidos com a reprodução em tanque de ondas de um tsunami. Para o primeiro *benchmark* o AnuGA apresentou uma maior aproximação à solução analítica que o COMCOT. Já no segundo *benchmark* os dois modelos obtiveram soluções muito próximas à solução experimental, o que indica que cumpriram os requisitos de validação.

Após a validação, foi realizado um primeiro caso de teste de inundação dos modelos. Foi escolhida a área de teste da Boca do Rio, um vale fluvial no Barlavento Algarvio relativamente próximo ao cabo de S. Vicente. Esta escolha deveu-se ao facto de existirem relatos históricos de observações ao tsunami de 1755, assim como ter sido identificada um depósito sedimentar marinho atribuído por Hindson e Andrade (1999) [16] ao mesmo tsunami. Este caso de teste teve como objectivo o de verificar a adaptação dos modelos à costa Algarvia, assim como a de testar diferentes configurações dos modelos e a sua influência na inundação. Foi seguida um método descrito no trabalho de Richardson *et al.* [33] onde este avalia o perigo de um tsunami similar ao de 1755 na costa da Grã-Bretanha. As configurações testadas incluíram no COMCOT o uso de equações lineares e não-

lineares para modelar a inundação e no AnuGA foi testada a alimentação, ou seja, o estabelecimento das condições iniciais a partir dos resultados dos modelos COMCOT e SWAN. Os resultados obtidos indicaram que não existiram diferenças significativas entre utilizar o SWAN ou o COMCOT como alimentação para o AnuGA. Quanto à inundação todas as configurações testadas obtiveram resultados semelhantes, excepto a utilização de equações lineares que previu resultados 50% superiores aos restantes. Ao serem comparados os resultados modelados com os dados históricos verificou-se uma boa aproximação do *run-up* sendo o *run-in* subestimado pelos modelos. No entanto, não existe a certeza de os relatos históricos serem 100% fiáveis sendo necessária alguma cautela quanto à sua análise.

Para efectuar a comparação sistemática da inundação foi escolhida a área de teste da baía do Alvor. Neste local é possível encontrar diversos ambientes morfológicos: duas barras de maré, a da Marina de Lagos junto à cidade de Lagos na zona oeste da área de estudo e a barra do Alvor que permite o acesso á laguna costeira "Ria de Alvor"; existem também zonas de praia com cordão dunar e ainda localidade junto à praia como Torralta ou Lagos. Foram criados 81 modelos de falha através da variação de dois parâmetros da falha: o ângulo de mergulho e a profundidade. Estes foram utilizados para criar as condições iniciais de propagação utilizando o método de Mansinha e Smylie (1971) [26] incorporado no software Mirone [24]. Foram efectuadas 81 corridas para cada modelo de tsunami e extraídos os parâmetros de inundação *run-up* e *run-in*. Ao sistematizar estes resultados em função dos parâmetros da falha: ângulo de mergulho e profundidade foi possível verificar que estes últimos têm diferente influência nos modelos. O AnuGA demonstrou maior capacidade para inundar com os modelos de falha com profundidades próximas aos 30 km enquanto que para o COMCOT foram os modelos de falha menos profundos que demonstram maior capacidade de inundar, no entanto o COMCOT mostrou ser mais variável que o AnuGA neste critério. Neste caso de teste foi igualmente comparada a alimentação do AnuGA para o modelo da falha que obteve a maior inundação e foi também efectuada uma comparação do efeito na propagação da onda da utilização entre uma batimetria de elevada resolução com origem em levantamentos multifeixe e uma batimetria com origem na digitalização de cartas náuticas do Instituto Hidrográfico.

Os resultados obtidos indicaram que a utilização do modelo SWAN para alimentar o AnuGA não apresenta diferenças significativas para a alimentação com COMCOT e permite que assim se compare a inundação obtida por AnuGA e COMCOT já que as condições de entrada dos modelos são semelhantes. Esta configuração apresenta ainda a vantagem de necessitar de um muito menor tempo de computação, cerca de 94% menos. A utilização de uma batimetria com origem em dados multifeixe não demonstrou provocar diferenças significativas na propagação da onda, no entanto, a zona onde esta está disponível não é muito acidentada. Os modelos COMCOT e AnuGA apresentaram resultados de propagação semelhantes sendo que as diferenças registadas nos parâmetros *run-up* e *run-in* são derivadas dos métodos de inundação. Este ponto levanta a questão de qual destes modelos melhor reproduz a realidade, sendo que esta questão não pode ser respondida apenas com recurso à análise de casos sintéticos.

Palavras-chave: *run-up* ; *run-in* ; comparação de modelos de tsunami; AnuGA; COMCOT

Acknowledgements

I would like to thank the support given by Professor Joaquim Luis and his availability to supervise the elaboration of the present thesis. His advices on technical and scientifical aspects of the work developed were crucial for its progess.

I would also like to acknowledge the support made available by the research project "Study on the Risk of Earthquakes and Tsunamis in the Algarve region" (ERSTA), a cooperation between University of Algarve and the Portuguese Civil Protection Authority, without which was impossible to develop this thesis.

I thank all my friends from the Oceanography course, from CIMA and all the others for the good times I have spent here so far and for the important part you have on this thesis.

I also like to thank Simon Connor for the precious, on the clock, english revisions and comments which have improved this work very much.

I thank and wish "um grande bem haja" to all my friends at Praceta da Amoreiras, Rinchoa city and Lisbon.

To Ana for being there when was needed and for motivating me to accomplish this work. Without you it was not possible to complete this work.

I dedicate this work to my family, my mother Noemia, my father Vitor and my grandmother Matilde. I love you.

Glossary

Fault Dip

Angle between the horizontal top surface and the fault plane

M_w

Moment Magnitude

Fault Strike

Angle measured clockwise from the North to the top edge of the fault plane

***Run-up* height**

The maximum height above the reference level at which the water reaches

***Run-in* length**

The maximum distance to the coastline of the flooded area

Acronyms

AnuGA

Australian National University/Geoscience Australia.

CFL

Courant-Friedrichs-Lewy condition.

COMCOT

Cornell Multi-grid Coupled Tsunami Model.

ERSTA

Tsunami and Earthquake Risk in the Algarve.

GMT

Generic Mapping Tools.

SWAN

Shallow Water Model.

UTM

Universal Transverse Mercator.

Contents

Abstract i

Resumo ii

Acknowledgements iv

Glossary v

Acronyms vi

1 Introduction 1

1.1 Scope of Work . . . 1
1.2 Recent History of Tsunami Research in Europe . . . 1
1.3 Numerical models in Tsunami research . . . 3
1.4 Structure . . . 4

2 Methods and Models 5

2.1 Numerical methods . . . 5
2.1.1 COMCOT . . . 6
2.1.2 AnuGA . . . 9
2.1.3 SWAN . . . 12
2.2 Methods description . . . 12
2.3 Validation . . . 13
2.3.1 Benchmark #1 - 2-D problem . . . 13
2.3.2 Benchmark #2 - run-up onto a 3-D beach . . . 14

3 Boca do Rio test case 17

3.1 Site description . . . 17
3.2 Historical data . . . 17
3.3 Source model . . . 19
3.4 Topographic and Bathymetric data . . . 20
3.4.1 Data sources . . . 20

3.4.2 Grid set-up . . . 21
3.5 Results . . . 23
3.5.1 AnuGA input comparison: COMCOT and SWAN . . . 23
3.5.2 Inundation: AnuGA and COMCOT . . . 25
3.5.3 Comparison with historical data . . . 27

4 Alvor test case **28**
4.1 Site description . . . 28
4.2 Source models . . . 29
4.3 Topographic and Bathymetric data . . . 31
4.3.1 Data sources . . . 31
4.3.2 Grid set-up . . . 32
4.4 Results . . . 33
4.4.1 AnuGA input comparison: COMCOT and SWAN . . . 34
4.4.2 Multibeam bathymetry usage . . . 37
4.4.3 Inundation modelling results . . . 40

5 Analysis **51**
5.1 Boca do Rio . . . 51
5.1.1 Model adjustment to the Algarve coast . . . 51
5.1.2 Model configurations . . . 51
5.2 Alvor . . . 52

6 Conclusion **53**

References **54**

Appendix A **a**

List of Figures

2.1 *COMCOT grid scheme (source: [1])* . . . 6
2.2 *Moving boundary illustration. (source: [1])* . . . 7
2.3 *Connecting boundary between 2 subregions.* . . . 8
2.4 *Piecewise linear reconstruction using centroids of the mesh. (source: [29])* . . . 11
2.5 *Benchmark #1 bathymetry contours* . . . 13
2.6 *Benchmark #2 bathymetry contours* . . . 14
2.7 *Catalina Benchmark 1, results for COMCOT and AnuGA.* . . . 15
2.8 *Catalina Benchmark 2, results for COMCOT and AnuGA.* . . . 16

3.1 *Boca do Rio study area* . . . 18
3.2 *Boca do Rio fault location and computed free surface elevation* . . . 19
3.3 *COMCOT grid set-up for the Boca do Rio test case. Figure extents represents the 1^{st} grid level, red rectangle is the 2^{nd} grid level and black rectangle is the 3^{rd} grid level.* . . . 21
3.4 *Topography used for AnuGA's mesh generation at Boca do Rio* . . . 22
3.5 *AnuGA grid set-up for the Boca do Rio test case.* . . . 22
3.6 *Water height comparison on western gauge at Boca do Rio* . . . 24
3.7 *Water levels comparison on southern gauge at Boca do Rio.* . . . 24
3.8 *Cross shore profile at Boca do Rio.* . . . 25
3.9 *Gauge and profile location at Boca do Rio. Water levels at gauge #6.* . . . 26
3.10 *Comparison of inundation extents at Boca do Rio.* . . . 27

4.1 *Study area of Alvor, aerial photography and grid image.* . . . 29
4.2 *Fault 9 localization* . . . 30
4.3 *Alvor study area data coverage* . . . 31
4.4 *Alvor grid coupling for the COMCOT model.* . . . 32
4.5 *AnuGA's digital terrain model regions at Alvor.* . . . 33
4.6 *Gauge and analysis zone locations at the Alvor study area.* . . . 34
4.7 *Wave gauge at the western boundary in Alvor* . . . 35
4.8 *Wave gauge at the southern boundary in Alvor* . . . 35
4.9 *Wave gauge at the eastern boundary in Alvor* . . . 36
4.10 *Wave gauges at the 5 m isobath in Alvor* . . . 36

4.11 *Multibeam and IH bathymetry grid difference.* 37
4.12 *Comparison of wave forms on two different bathymetries with AnuGA model.* 38
4.13 *Comparison of wave forms on two different bathymetries with COMCOT model.* 39
4.14 *Run-up at the West/Lagos zone. (a) AnuGA e (b) COMCOT. In this figure we plot contours of the maximum water height at the West/Lagos zone in function of source parameters: dip on the horizontal axis and depth on the vertical axis. (see figure 4.6 for zone bounds).* . . 40
4.15 *Run-up at the Central/Ria zone. (a) AnuGA e (b) COMCOT. (see figure 4.6 for zone bounds).* 41
4.16 *Run-up at the East/Alvor zone. (a) AnuGA e (b) COMCOT. (see figure 4.6 for zone bounds).* 41
4.17 *AnuGA and COMCOT comparison for the highest run-up attained with AnuGA.* 43
4.18 *AnuGA and COMCOT comparison for the highest run-up attained with COMCOT.* . . . 44
4.19 *Run-in results for the West/Lagos zone, Meia-Praia area.* 45
4.20 *Run-in results for the West/Lagos zone, Marina area.* 45
4.21 *Run-in results for the Central/Ria zone.* 46
4.22 *Run-in results for the East/Alvor zone.* 47
4.23 *Amplification factors.* 48
4.24 *AnuGA and COMCOT comparison in AnuGA's highest run-in case.* 49
4.25 *AnuGA and COMCOT comparison in COMCOT's highest run-in case.* 50

List of Tables

3.1 *Wave parameters from historical reports* 18
3.2 *Boca do Rio source model parameters* 19
3.3 *Summary of the modelled inundation results with the four configurations.* 26
3.4 *Summary of the data obtained from historical reports.* 27

4.1 *Alvor's test case source model parameters* 30
4.2 *AnuGA maximum water heights at the boundary and 5 m isobath gauges.* 38
4.3 *COMCOT maximum water heights at the boundaries and 5 m isobath gauges.* 39
4.4 *Highest run-up in each analysis zone of Alvor.* 42
4.5 *Highest run-in for each analysis zone at Alvor.* 47

Chapter 1

Introduction

1.1 Scope of Work

The present work was developed in connection with the work activities of task: "WP3: Test of numerical models" of the ERSTA investigation project "Tsunami and Earthquake Risk in the Algarve", a cooperation between the National Civil Protection Authority and the University of the Algarve.

The author of this thesis collaborated with the team carrying out the above research project. Therefore, the analysis presented here was performed taking advantage of the datasets of the ERSTA project.

The ERSTA project is aimed at gathering knowledge of the Algarve's vulnerability to earthquakes and tsunamis, the risk of those threats and their estimated damage in order to develop dedicated emergency planning and policies of prevention and protection. All of the technical and scientific results are to be compiled in a simulator for visualization and estimation of damage. A numerical model of tsunami propagation and inundation is to be included in the simulator. The objective of task WP3 and this work was to compare the propagation and inundation results of various numerical models.

To accomplish this objective we installed three numerical models in conditions adapted to the Algarve coast. Comparison of the models was based on the *run-up* and *run-in* parameters derived from the results obtained.

1.2 Recent History of Tsunami Research in Europe

Contemporary tsunami research in Europe began approximately 50 years ago, following the 1956 Aegian Sea tsunami, which originated close to the islands of Amorgos and Astipalaia[39]. At the same time there was also a growing interest in tsunami research in the main countries on the Pacific Rim (USA, USSR and Japan). This growth was a result of two destructive tsunamis: the 1946 Alaska-generated tsunami that killed 173 in Hawaii, and the 1960 Chilean tsunami that killed 1000 people in Chile, 61 in Hawaii and 199 in Japan [11, 39]. These events led to the establishment of a Warning System in the Pacific and the creation of two organizations (the International Tsunami Commission in 1960 and the International Coordinating Group for Tsunami Warning System in the

Pacific a few years later), representing science and government, in an international effort to mitigate against tsunami impacts [11, 39].

However, European research interest rapidly declined, disappearing almost completely from the international scene until the end of the '80s, when the International Working Group on tsunamis was created [39]. An important project at the time, involving several partners in Europe, was named "Genesis and Impacts of Tsunamis on the European Coasts" (GITEC: described in Tinti (1993) [39]). GITEC was carried out between 1992 and 1995 with the aim of contributing to the reduction of hazard and risk associated with tsunamis in European countries. This project was followed by GITEC-TWO between 1996 and 1998. These projects have produced several publications. The most important for the current research have been the works of Baptista *et al.* [7, 8] that address the 1755 Lisbon tsunami and its possible sources. In addition, tsunami catalogues (such as Papadopoulos (1998) [32] for Greece and adjacent seas as well as a unified catalogue for Europe from Tinti *et al.* (1998) [40]) were produced and published.

More recently, the Sumatra tsunami disaster of December 2004 has drawn the attention of the general public and authorities worldwide to the destructive impact that a tsunami can have [6, 11, 13]. This event has given new impetus to tsunami research, with a focus on establishing warning systems. A few days after the tragedy which had struck South Asia, the European Union (EU) Council of Ministers decided to examine ways of improving the EU's Civil Protection Mechanisms and to investigate the possibility of developing an EU rapid reaction capability to deal with disasters [13].

At a policy level, the nations present at the World Conference on Disaster Reduction, held in Hyogo, Japan in January 2005, agreed on the "Hyogo Framework for Action 2005-2015: Building the Resilience of Nations and Communities to Disasters" [28]. Which calls upon regional organizations with a role related to risk reduction to, as stated, "Support the development of regional mechanisms and capacities for early warning to disasters, including tsunami"[12, 28]. At the same time the European Union disclosed its Tsunami Action Plan, in which it stated that "proposals should cover the establishment of detection and early warning systems (EWS) for the Indian Ocean, as well as for the Mediterranean and the Atlantic"[12].

With the intention of improving EWS, the European Commission has funded several research projects between 2006 and 2009. Projects focussed on the Mediterranean region are: *a*) "Seismic eArly warning For EuRope" (SAFER), which aims at developing tools for effective earthquake early warning in Europe[4]; *b*) "SEismic and tsunami risk Assessment and mitigation scenarios in the western HELLenic ARC" (SEAHELLARC), whose objectives are to establish a real-time network for seismic and tsunami observations and develop methodologies and tools for the protection of coastal areas [3]; *c*) "Integrated observations from NEAR shore sourcES of Tsunamis: towards and early warning system" (NEAREST), which addresses potential near-shore tsunami sources in the Gulf of Cadiz for the improvement of near-real time detection of signals to be used in the EWS prototype, the improvement of numerical models for study of tsunami impact and production of accurate maps [2]; and *d*) "Tsunami Risk ANd Stratagies For the European Region" (TRANSFER), which aims at improving present knowledge of tsunami processes, particularly in the seas surround-

ing Europe [5]. The latter project and ERSTA have collaborated during the past two years.

National projects without the EU support have also developed over recent years. In the United Kingdom (UK), the Department for Environment, Food and Rural Affairs (DEFRA) began by commissioning a study in early 2005 to investigate the threat posed by tsunamis to the UK [19]. The study results indicated that the most likely scenario, for a significantly damaging tsunami would arise from a large, relatively close earthquake, producing a tsunami whose effects would be severe only locally. It also identified tsunami sources that have impacted on the UK coast in the past, specifically the earthquake of 1755. In August 2005, a second study was commissioned by DEFRA with the objectives of refining of the potential impact of events similar to the 1755 earthquake and tsunami, called "Lisbon-type events", and investigate impacts of near-coast events, namely in the North Sea [33].

In Portugal, the first study to identify seismic risk used the metropolitan area of Lisbon as a case study. The 1755 earthquake and tsunami that devastated Lisbon are embedded in Portuguese collective memory even today. This study was commissioned by the Portuguese Civil Protection (ANPC) in 1998 [31]. A second study was commissioned in 2006 by ANPC, this time with the Algarve region as case study. Since the Algarve and Lisbon are both areas of intensity X in the Modified Mercalli scale [31]. This project goes by the name of "Study on the Risk of Earthquakes and Tsunamis in the Algarve region" and has the acronym ERSTA in Portuguese.

1.3 Numerical models in Tsunami research

In recent research developed in Portugal or by European partners, the most commonly used numerical codes for tsunami simulation have been SWAN from Mader [25], TUNAMI-N2 from Inamura [18], MOST from the National Oceanic and Atmospheric Administration (NOAA) [41] and COMCOT from the University of Cornell [22].

The SWAN model has been used in the works of Baptista *et al.* [8–10], but this code is not able to model inundation by itself and so has been used for direct analysis of wave heights near the coast and arrival times [8, 9], or to feed other numerical codes capable of modelling inundation [10]. The TUNAMI-N2 code has primarily been used for modelling inundation in the works of Baptista *et al.* [10] and Silva [36] and is integrated in the software Mirone [24] used in this work. Nevertheless, the version available is limited by not using coupled terrain models (only allowing for one spatial resolution of the study area) and not including momentum as an initial condition. Hence, we have not considered this code for the purposes of our work. The MOST and COMCOT codes are being used in the project TRANSFER [5]. Unfortunately, the former was not available to our project and it was not possible to use it. The latter has been used to investigate historical tsunamis like the 1960 Chilean Tsunami [21] and, more recently, the 2004 Sumatra-Andaman Tsunami [43]. The COMCOT model has a free code licence and can be obtained on the internet (http://ceeserver.cee.cornell.edu/pll-group/comcot.htm). A more recent nu-

merical code named AnuGA, has been developed by Australian National University (ANU) and Geoscience Australia (GA) [30] and is being used in the establishment of the Australian Tsunami Warning System [34]. This code is also released under a free licence and available on the internet (http://sourceforge.net/projects/anuga). Another numerical code available to the project was the CLAWPACK model developed originally by LeVeque [20] and later modified by George [15] for the purpose of tsunami modelling. We ruled out its use in this project because the adaptive mesh refinement algorithm allowed less control of detailed areas than the required by the ERSTA project.

Therefore, the numerical tsunami modelling codes evaluated in this work are AnuGA, with possible initial conditions imposed from SWAN or COMCOT, and COMCOT.

1.4 Structure

This thesis is structured in 6 chapters. The following chapter introduces the numerical theory that is the basis of the codes evaluated. Next, it outlines the methods used for code validation and for the test cases. In the end of the chapter a description and the presentation of the validation process results is made.

Chapter 3 describes the Boca do Rio test case. Starting with the study area location and description, introduces the historical data collected, describes the source model used and the datasets used for the digital terrain models. In the the final section the results are presented and an analysis is made.

Chapter 4 describes the Alvor test case. Starts with an outline of study area location and morphology, followed by a description of the source models used and methods for the digital terrain model creation. The last section presents the results of the test case and an analysis is made.

Chapter 5 makes an analysis of all the results obtained in the work. The final chapter integrates these results and proposes directions for further research.

Chapter 2

Methods and Models

This chapter will begin by briefly reviewing the theory behind the numerical models used in this work. Next, the methods used and the structure of the work will be described. At the end of the chapter a theoretical validation of the models to be used will be presented, along with the results achieved.

2.1 Numerical methods

The numerical models used during the study were the COrnell Multi-grid COupled Tsunami model [22] from Cornell University USA, referred as COMCOT, the ANU/Geoscience Australia tsunami inundation model, referred as ANUGA [30] and SWAN developed by Mader Consulting[25].

The models were developed based on non linear shallow water wave equations (NLSWE), equations (2.1), (2.2) and (2.3). With COMCOT it is possible to use a spherical coordinate system allowing transoceanic propagation and also a Cartesian coordinate system for smaller scale computation [22]. On the other hand, AnuGA uses SWE with spatial coordinates in the Universal Transverse Mercator (UTM) Cartesian system [29]. For the purpose of the work developed, both models were set-up using the UTM system, since the source locations and the study site locations are less than 6 degrees apart and hence there is no need for transoceanic propagation.

Equations (2.1), (2.2) and (2.3) are the NLSWE where ζ is the free surface elevation, P and Q are the horizontal discharge ($P = Hu_x$ and $Q = Hu_y$), H is the total water depth and τ_x and τ_y the friction coefficients.

$$\frac{\partial \zeta}{\partial t} + \frac{\partial P}{\partial x} + \frac{\partial Q}{\partial y} = 0 \tag{2.1}$$

$$\frac{\partial P}{\partial t} + \frac{\partial}{\partial x}\left(\frac{P^2}{H}\right) + \frac{\partial}{\partial y}\left(\frac{PQ}{H}\right) + gH\frac{\partial \zeta}{\partial x} + \frac{\tau_x H}{\rho} = 0 \tag{2.2}$$

$$\frac{\partial Q}{\partial t} + \frac{\partial}{\partial x}\left(\frac{PQ}{H}\right) + \frac{\partial}{\partial y}\left(\frac{Q^2}{H}\right) + gH\frac{\partial \zeta}{\partial y} + \frac{\tau_y H}{\rho} = 0 \tag{2.3}$$

2.1.1 COMCOT

COMCOT offers the possibility of using the linear Boussinesq equation including the Coriolis force (Inamura *et. al.* (1988) and Liu *et. al.* (1994) in [22]) for simulating distant propagation, since the wave slope is small outside the continental shelves making the non-linear convective inertia force not significant and can therefore be ignored [22]. However, this assumption is no longer valid as the tsunami propagates into shallower water and the wave amplitude increases and the wave length diminishes due to shoaling effects on the continental shelf. In this situation, the non-linear SWE including bottom friction should be used in the modelling of tsunami inundation.

The discretization of the linear model is done using an explicit staggered leap-frog finite difference method. According to the authors this scheme solutions satisfies the linear Boussinesq equations up to the third order in terms of the grid size [22]. The method proposed calculates the free surface displacement at the centre of every grid point on the $(n + \frac{1}{2})$th time step, the volume flux components are evaluated at the surrounding grid points, as shown in figure 2.1.

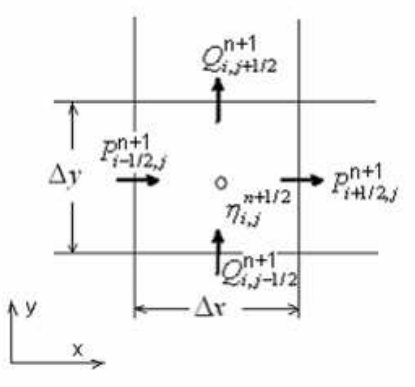

Figure 2.1: *COMCOT grid scheme (source: [1])*

Non-linear SWE can be written in the form of the equations (2.1), (2.2) and (2.3); the linear terms are discretized using the same leap-frog finite difference scheme and the non-linear advective terms are discretized with an upwind scheme [22]. The upwind scheme is conditionally stable and introduces some numerical dissipation [22], but if the velocity gradient in the fluid field is not too steep and the CFL (Courant-Friedrichs-Lewy) condition [14] is satisfied, the upwind formulation is preferred due to its small computational effort [22].

The non-linear formulation includes the bottom shear stress terms, modelled with the Manning's formula, equations (2.4) and (2.5), where n represents the Manning's relative roughness coefficient,

$$\tau_x = \frac{\rho g n^2}{H^{\frac{7}{3}}} P \left(P^2 + Q^2\right)^{\frac{1}{2}} \tag{2.4}$$

$$\tau_y = \frac{\rho g n^2}{H^{\frac{7}{3}}} Q \left(P^2 + Q^2\right)^{\frac{1}{2}} \tag{2.5}$$

Inundation - Moving boundary scheme

To model run-up and run-down a moving boundary scheme is used. The shoreline is defined as the interface between a dry and a wet cell, and the volume flux normal to the interface is assigned to zero.

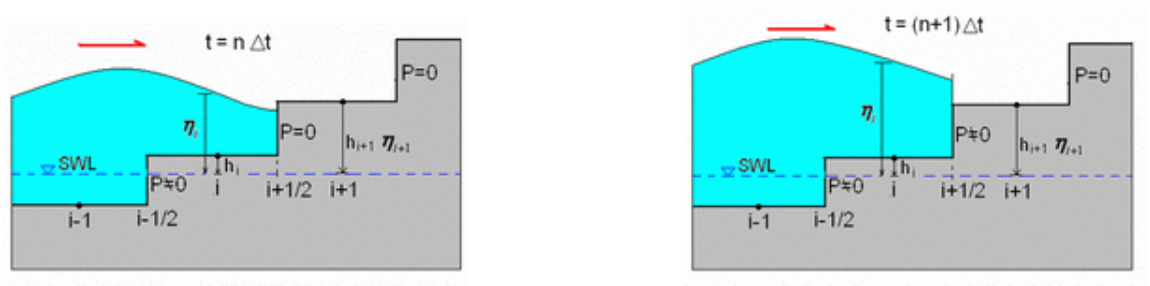

Figure 2.2: *Moving boundary illustration. (source: [1])*

The above image, figure 2.2, illustrates the algorithm. It is applied when $\eta_i > 0$ and $\eta_{i+1} \leq 0$. On the left side image, $h_{i+1} + \eta_i < 0$ and the shoreline stays at i+1 and $P_{i+\frac{1}{2}} = 0$. On the right hand side image, $h_{i+1} + \eta_i > 0$ so the shoreline moves between cell i+1 and cell i+2. The total water depth at cell i+1 is now $H = h_{i+1} + \eta_i$.

Connecting boundary condition

COMCOT uses a nested multi-grid two-way coupling method that allows different grid size and time step size to be employed in different sub-regions in order to adequately model frequency dispersion and obtain detailed information in the coastal region [22].

With a two-way coupling method the free surface elevation values from the inner region are used to update the outer region and the outer region volume flux values are used to update the inner region ones. The latter is accomplished by linearly interpolating the neighbouring volume fluxes from the large grid system to the small grid system over a larger time interval, since the time step of the smaller region is half of the larger region in order to satisfy the CFL condition [22].

Knowing the all the fluxes at time step $t = t_1$, the following nine steps are necessary in order to solve all the fluxes at the next time step $t = t_2$. The time step of the inner region is half of the outer region, for reference of the connecting boundary see figure 2.3.

1. Calculate the free surface elevation at $t_{i+\frac{1}{2}}$ in the outer region by solving the continuity equation;

2. The fluxes at t_1 in the outer grid at the connected boundary are linearly interpolated and the values assigned to the flux in the inner region at the boundary. Solve the continuity equation at the inner grid;

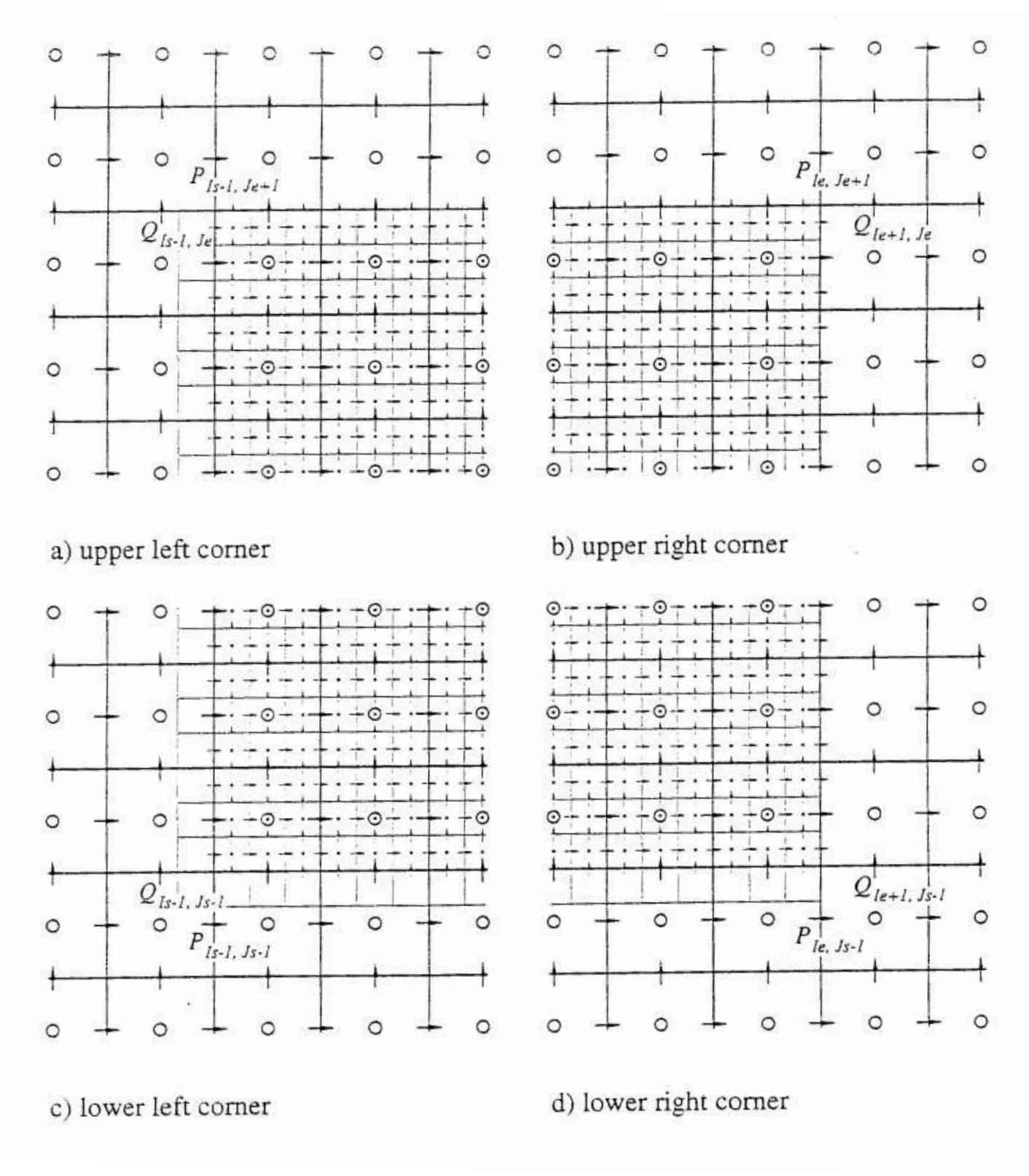

Figure 2.3: *Connecting boundary between two subregions. (Adapted from [22]).*

3. Obtain the free surface elevation at $t_{1+\frac{1}{4}}$ in the inner region by solving the continuity equation;

4. Obtain the flux at $t_{1+\frac{1}{2}}$ in the inner region by solving the momentum equation;

5. In order to calculate the free surface elevation in the inner region at $t_{1+\frac{3}{4}}$, the flux at the connected boundary at $t_{1+\frac{1}{2}}$ is required. First, using the free surface elevation $t_{1+\frac{1}{2}}$ and the flux t_1 in the outer region, the flux in the outer region along the connected boundary at t_2 is obtained by solving the linear momentum equation locally. Second, these flux values at t_2 are linearly interpolated along the connected boundary. To get the flux values at $t_{1+\frac{1}{2}}$, outer flux at t_1 and t_2 are time-averaged. Those spatially and temporally averaged flux values are assigned to the flux in the inner grid at the boundary;

6. Obtain the free surface elevation at $t_{1+\frac{3}{4}}$ in the inner region by solving the continuity equation;

7. To transfer the information from the inner to the outer region, the free surface elevation in the inner region is spatially averaged over the grid size of the outer region. These averaged values at $t_{1+\frac{3}{4}}$ are then time-averaged with those at $t_{1+\frac{1}{4}}$ in the inner region. These spatially and averaged elevation values in the inner region update the elevation values at $t_{1+\frac{1}{2}}$ in the outer region;

8. Obtain the flux values at t_2 in the inner region by solving the momentum equation;

9. Obtain the flux values at t_2 in the outer region by solving the momentum equation;

2.1.2 AnuGA

AnuGA uses a mesh composed of triangular cells to represent the study area. Cell sizes may be varied within the mesh to allow greater resolutions in areas of interest. The triangles are obtained with a Delaunay triangulation [35] which has the property that no vertex in the vertex set falls in the interior of the circumcircle (circle that passes through all three vertices) of any triangle in the triangulation.

The NLSWE used are the system of differential conservation equation in the form of equation 2.6.

$$\frac{\partial U}{\partial t} + \frac{\partial E}{\partial x} + \frac{\partial G}{\partial y} = S \tag{2.6}$$

Where $U = [h\ uh\ vh]^T$ is a vector of conserved quantities: water depth h, x momentum uh and y momentum vh. Other quantities entering the system are bed elevation z and stage or the absolute water level w. The relation $w = z + h$ holds true at all times. The fluxes in the x and y direction, E and G are given by 2.7 and 2.8.

$$E = \begin{bmatrix} uh \\ u^2h + gh^2/2 \\ uvh \end{bmatrix} \tag{2.7}$$

$$G = \begin{bmatrix} vh \\ vuh \\ v^2h + gh^2/2 \end{bmatrix} \tag{2.8}$$

The source term S which includes gravity and friction is given by equation 2.9; where S_0 is the bed slope and S_f is the bed friction, modelled using Manning's resistance law [30].

$$S = \begin{bmatrix} 0 \\ gh(S_{0x} - S_{fx}) \\ gh(S_{0y} - S_{fy}) \end{bmatrix} \tag{2.9}$$

In each triangle, the conserved quantities, water depth (h) and the horizontal momentum (uh, vh) are updated, using a finite volume method (FV). Equation (2.10) describes the rate of change of the average of the conserved quantities within each cell, obtained by applying the divergence theorem to the integration of the differential SWE [30].

$$A_i \frac{dU_i}{dt} + \sum_j (F_{ij} n_{ij1} + G_{ij} n_{ij2}) l_{ij} = A_i S_i \tag{2.10}$$

Where the i refers to the ith cell, A_i is the cell area, U_i is the vector of the averaged conserved quantities and S_i the source term associated with each cell, which includes gravity and friction. The notation $F_{ij} n_{ij1} + G_{ij} n_{ij2}$ is used to denote the approximation of the outward normal flux of material across the ijth edge and l_{ij} is the length of the corresponding edge.

Setting the initial values for any quantity can take a variety of forms which include constants, linear combinations of other quantities and arbitrary functions f(x,y). The source data can also take the form of an arbitrary set of points with associated values. The points need not to coincide with the mesh triangle vertices or centroids; a penalized least squares technique is employed to populate the quantity in a smooth and stable way [30].

From the values of the conserved quantities at the centroids of each cell and its neighbouring cell, a discontinuous piecewise linear reconstruction of the conserved quantities is obtained (figure 2.4). The function is allowed to be discontinuous at the edges but the slope is limited to avoid unnecessary oscillations. A multidimensional slope-limiting technique is employed to achieve second-order spatial accuracy and prevent oscillations [29].

The friction term is included in the source terms and modelled using Manning's formula, equations (2.4) and (2.5). The time discretization is made using an explicit Euler time stepping method

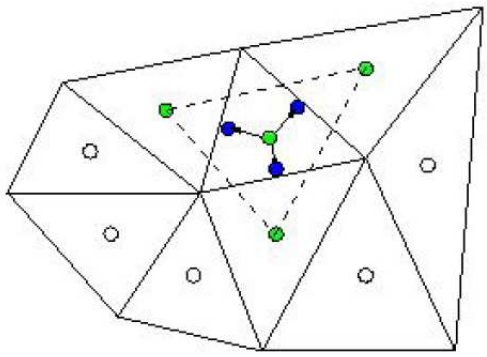

Figure 2.4: *Piecewise linear reconstruction using centroids of the mesh. (source: [29])*

[44] with variable time steps adapted to satisfy the CFL condition.

Boundary conditions

Model AnuGA provides several predefined boundary conditions but also allows the user to define his or her own boundary conditions following the specifications. In this section we will only overview the available boundary conditions.

In AnuGA the boundaries are specified using tags. In the mesh there is a list that identifies the boundary triangles and associates a tag with each [29]. The user assigns a boundary condition to each tag. The following predefined boundary conditions are available:

- **Reflective boundary**: returns the same stage in its neighbouring volume but with the momentum reversed;
- **Transmissive boundary**: returns the same conserved quantity as those present in its neighbouring volume, which is a way of modelling outflow from the domain;
- **Dirichelet boundary**: specifies a constant value for stage and momentum;
- **Time boundary**: specifies the stage and momentum according to time varying function;
- **File boundary**: allows the user to supply a file containing the stage and momentum or a time series to the boundary segment. The boundary values are interpolated to the appropriate segments;
- **Field boundary**: the same as File boundary but allows the user to change the level of the stage height. It is useful when running the same input but with different tide heights;
- **Transmissive momentum set stage boundary**: returns the momentum quantities as those present in its neighbour volume but sets stage as in Time boundary. It is useful when stage is known at the boundary but the momentum is not;

2.1.3 SWAN

The SWAN numerical model developed by Mader Consulting Co. [25] is currently one of the most widely used in tsunami studies [9, 10].

The model solves the non-linear shallow water (NLSW) long wave equations using the finite difference numerical scheme. The equations are solved in the Cartesian coordinate system and include the Coriolis effect.

According to the author, the model is suitable for tsunami wave formation, propagation and the initial behaviour of shoaling. Its main limitations are inundation modelling and source modelling.

In the scope of the work developed, the model was used for propagation from the source to the near shore, on the continental shelf. With SWAN, it is possible to quickly obtain a free surface variation, and horizontal momentum as a function of time. These results were used to input into AnuGA's boundaries as initial values for its runs.

The advantages of using SWAN input to initialize AnuGA include the less computational effort needed and the fact that no data processing is needed if the software Mirone [24] is used, since it is able to output results in a suitable format for AnuGA. Disadvantages include the limitation of SWAN only allowing one digital model terrain for propagation modelling where a low resolution has to be used.

2.2 Methods description

This section presents a description of the methods used in this work. In order to accomplish the proposed objectives, each step taken has a motivation and an aim to fulfil. These will be presented next.

The first step performed was the validation of the numerical models used. Validation is the process that ensures model performs well in a wide range of circumstances and is accomplished through comparison with analytical solutions. Validated codes also largely reduce the level of uncertainty in their results to the uncertainty in the initial geophysical conditions [38]. There are four types of validation data: *a*) basic hydrodynamic considerations; *b*) analytical benchmarks; *c*) laboratory benchmarks; and *d*) field benchmarks. In this work we have used the benchmarks proposed at the 2004 Catalina Long Wave Congress [42] which cover types *b)* and *c)* and will be presented in this chapter.

After the validation process we performed a test case at Boca do Rio based on the method of a Lisbon type event described in the work of Richardson *et. al.* (2006)[33]. Their study is an evaluation of the hazard of tsunamis for the UK and Irish coasts. Part of the study is related to the hazard of an event similar to the 1755 Lisbon tsunami, for which the authors investigated possible sources of the tsunami and used numerical models to assess water heights near the coast and calculate the level of hazard. In our work we have used one of the proposed tsunamigenic sources of

Richardson *et. al.* (2006) and available historical reports of the 1755 tsunami event at Boca do Rio in order to model an event of similar intensity. The purpose of this test case is to test both models' configurations and compare the results with historical data in order to assess their reliability.

The final step to fulfil the proposed objectives was to intensively test the numerical models properly configured after the Boca do Rio test case. For that purpose a range of fault models were obtained from varying two fault parameters: fault dip and depth. Comparison was made from the inundation parameters: *run-up* , *run-in* and amplification factor; which were derived from the inundation modelling performed. Taking advantage of having a multibeam bathymetric dataset, we also tested the effect of using this dataset against a bathymetric dataset developed from digitized nautical charts.

2.3 Validation

The two benchmarks used in the numerical model validation process were proposed at the 2004 Catalina Long Wave Congress [42]. The first is a 2-D problem on the vertical plane with an analytical solution. The second is the reproduction of the 1/400 scale laboratory experiment of the Monai run-up due to the 1993 Okushiri tsunami.

2.3.1 Benchmark #1 - 2-D problem

The topography of the problem consists on a 1/10 uniformly sloping beach (figure 2.5) with an initial free surface elevation given. The purpose is to calculate the shoreline trajectory for the running time and plot snapshots of the water surface at $t = 160s$, $t = 170s$ and $t = 220s$.

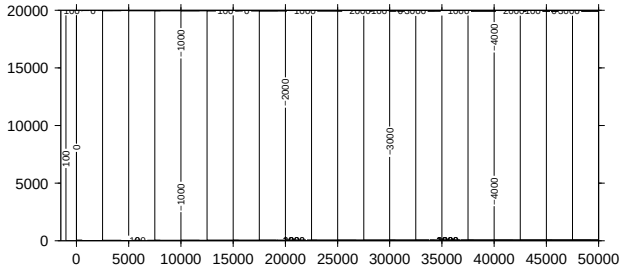

Figure 2.5: *Benchmark #1 bathymetry contours*

The results obtained for the first benchmark (figure 2.7) show differences in the shoreline evolution between the models. COMCOT has a bigger deviation from the analytical solution than AnuGA. A linear correlation coefficient (r) between each model and the analytical solution verifies this observation. The linear correlation between COMCOT and the solution is of 0.88 while between AnuGA and the solution this value is of 0.95. This observation holds for all the free surface

snapshots, where AnuGA presents a solution closer to the analytical result than COMCOT.

2.3.2 Benchmark #2 - run-up onto a 3-D beach

The second benchmark is the modelling of a 1:400 scale laboratory experiment using a large scale tank with a length of 205 m, width of 3.4 m and depth of 6 m performed by [27]. Figure 2.6 represents the bathymetry contours used in the experiment. The purpose is to model the free surface elevation and output the results in three gauges near shore. The gauges are placed in the following positions:

- point 4.521, 1.196 named "Gauge 5";
- point 4.521, 1.696 named "Gauge 7";
- point 4.521, 2.196 named "Gauge 9";

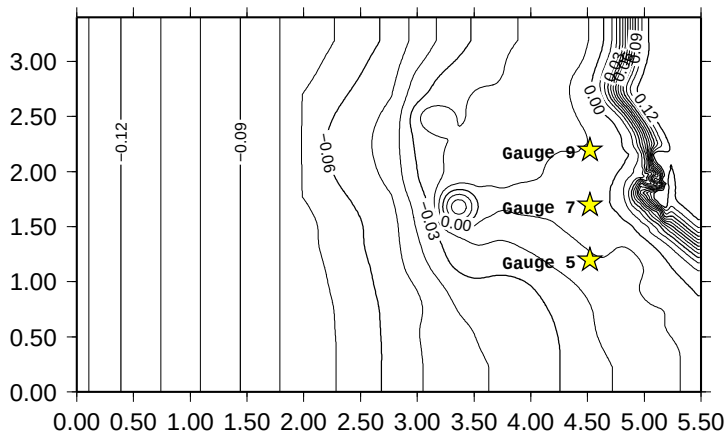

Figure 2.6: *Benchmark #2 bathymetry contours*

For the second benchmark results we have also examined the linear correlations coefficients between the models and the experimental data. Figure 2.8 shows the plots from gauges 5, 7 and 9 where we can observe that in this benchmark the results between the models and the experimental data are much closer than in the previous benchmark. Linear correlations confirm this observation since AnuGA obtains correlations of 0.94, 0.86 and 0.98 respectively and for COMCOT these values are 0.94, 0.85 and 0.97 respectively.

The differences in the maximum wave heights of the modelled results recorded on the gauges range from approximately -4 to +7% of the experimental data maximum. The maximum time lag in the occurrence of maxima and minima between the modelled results and the experimental data is of 1.9 s and occurs on gauge 7 with COMCOT model.

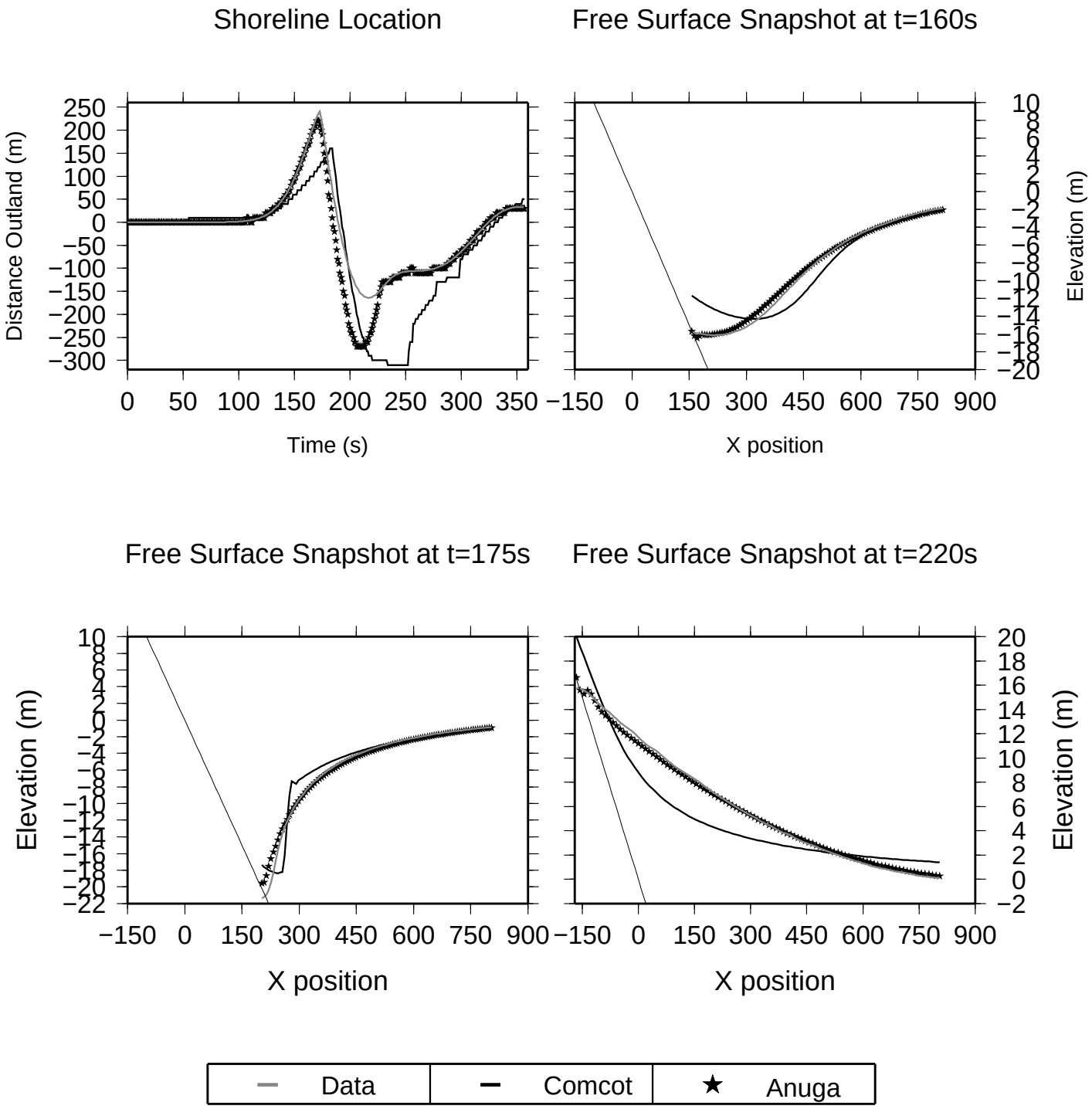

Figure 2.7: *Catalina Benchmark 1, results for COMCOT and AnuGA.*

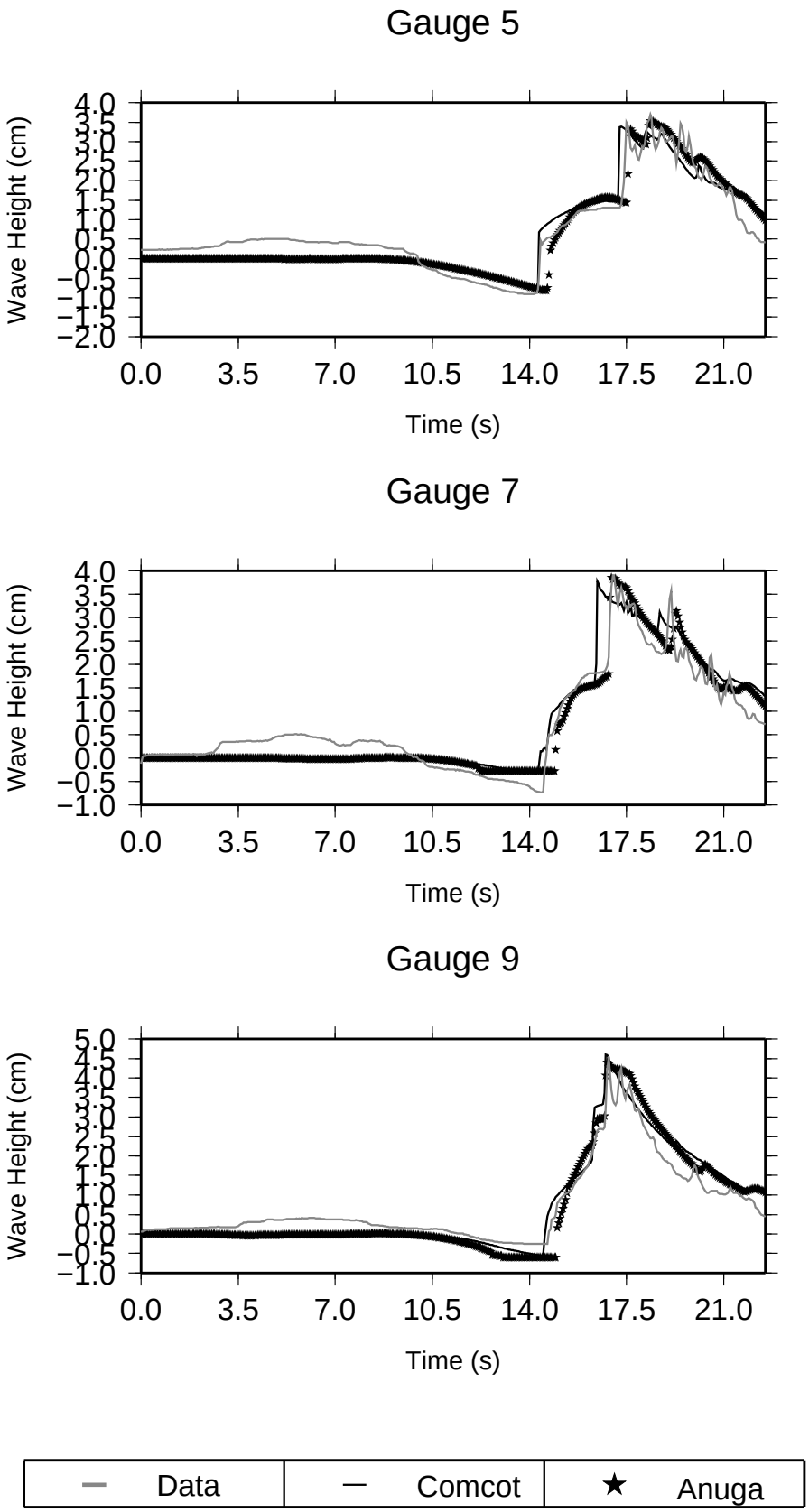

Figure 2.8: *Catalina Benchmark 2, results for COMCOT and AnuGA.*

Chapter 3

Boca do Rio test case

As described in section 2.2 the Boca do Rio test case aims to modell an event similar to the 1755 Lisbon tsunami using one of the tsunamigenic sources proposed by Richardson *et. al.* (2006) [33]. We intend to adjust the model's runs to the Algarve coast with a simple configuration at a test site with historical and sedimentological information is available [16, 17, 23, 37].

With the set-up to be described in this chapter, we expect to be able to: *a*) compare COMCOT's configurations using linear or non-linear equations in modelling inundation with the historical data; and *b*) to compare the effect of using SWAN or COMCOT as initial conditions for AnuGA's runs.

This chapter begins by describing the location of the Boca do Rio valley and introducing the compilation of the historical data. Next, we overview the choices made regarding source parameters used as input for the numerical models. Afterwards, a summary is made of the topographic and bathymetric data sources and the methods for creating numerical grids used on the runs. Finally, an analysis of the results achieved for each configuration used is compared with historical data.

3.1 Site description

Figure 3.1 illustrates the area of the Boca do Rio valley, a small estuary surrounded by rocky cliffs. This lowland consists of a flood plain formed by three small rivers: the *Ribeira de Budens*, *Ribeira de Boi* and *Ribeira de Vale Barão*. It is separated from the sea by a sandy barrier orientated from west to east.

The Boca do Rio valley is considered a good test case for two main reasons: firstly due to the availability of historical reports on the 1755 Lisbon tsunami [23, 37], and secondly a tsunami sedimentary deposit attributed to the same tsunami has been identified and defined through several drills at Boca do Rio [16, 17].

3.2 Historical data

The Historical reports of the 1755 Tsunami were gathered and compiled by authors Lopes (1841) and Pereira de Sousa (1919) in Hindson & Andrade (1999) [16]. The following citation summarizes the effects reported at Boca do Rio: "...Through the fresh water creek on the day of the earthquake,

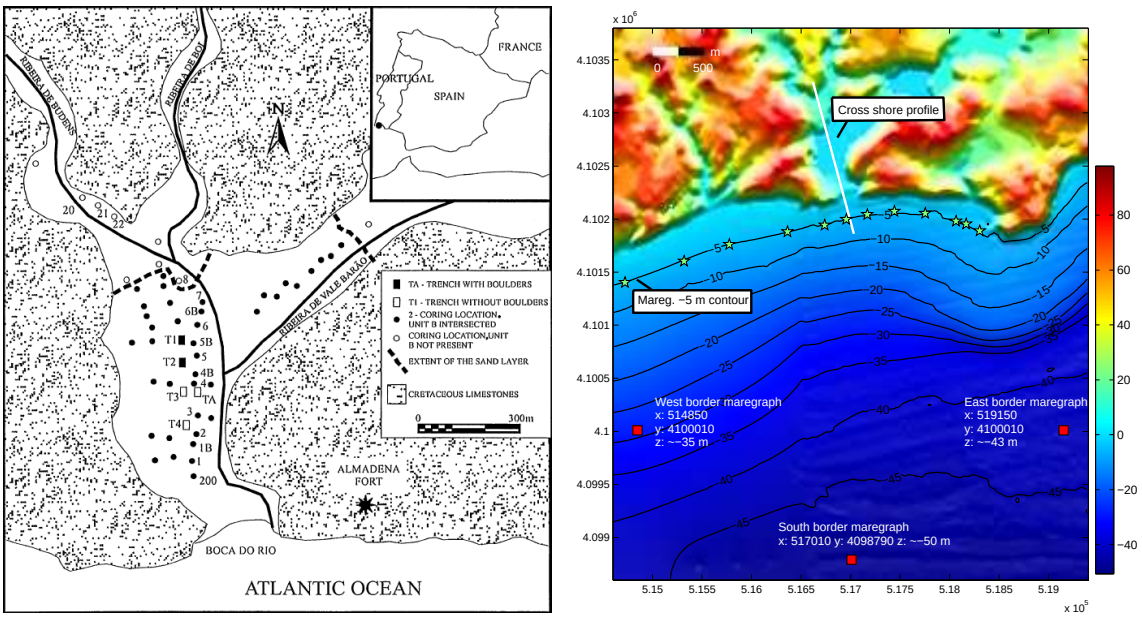

(a) (b)

Figure 3.1: *Detailed Boca do Rio study area images. (a) Map of the estuarine plain with geological units, adapted from [16]. Dashed line indicates the extent of the 1755 tsunami deposit.(b) Colour image of the bathymetric grid used in the models with tide gauges and profile used.*

the sea has entered in a distance of $\frac{1}{2}$ *légua* [approximately 2500 m] with a height of 10 to 12 *varas* [approx. 11 to 13 m], dragging large quantities of sand and transporting 50 anchors more than $\frac{1}{4}$ of a *légua* [approx. 1250 m] inland...".

From the report, it was possible to identify the maximum observed wave height and maximum observed *run-in* distance, one *légua* is approximately 5500 m and one *vara* is 1.1 m. The identified parameters are summarized in table 3.1.

	max. *run-up* (m)	max. *run-in* (m)
Boca do Rio	11 to 13	2500

Table 3.1: *Observed wave parameters inferred from the historical reports at Boca do Rio.*

According to authors [16, 17] the sedimentary paleo-deposits identified at Boca do Rio are of tsunamigenic origin and attributed to the 1755 event. We have georeferenced figure 3.1a into the UTM Cartesian system with the help of aerial photography of the study site in the software Mirone [24] and have been able to derive the extents of the sedimentary sand deposit identified by dashed lines.

3.3 Source model

The source mechanism of the 1755 Lisbon earthquake is not yet fully understood. Conflicting information and large uncertainties lead to several possibilities for epicentres spanning around 500 km of the Gorringe Bank area [8, 9, 33].

For the purposes of our work, we have used one of the sources proposed in the Richardson *et. al.* report [33], in which possible sources have been identified and used for simulation of an event similar to the 1755 tsunami.

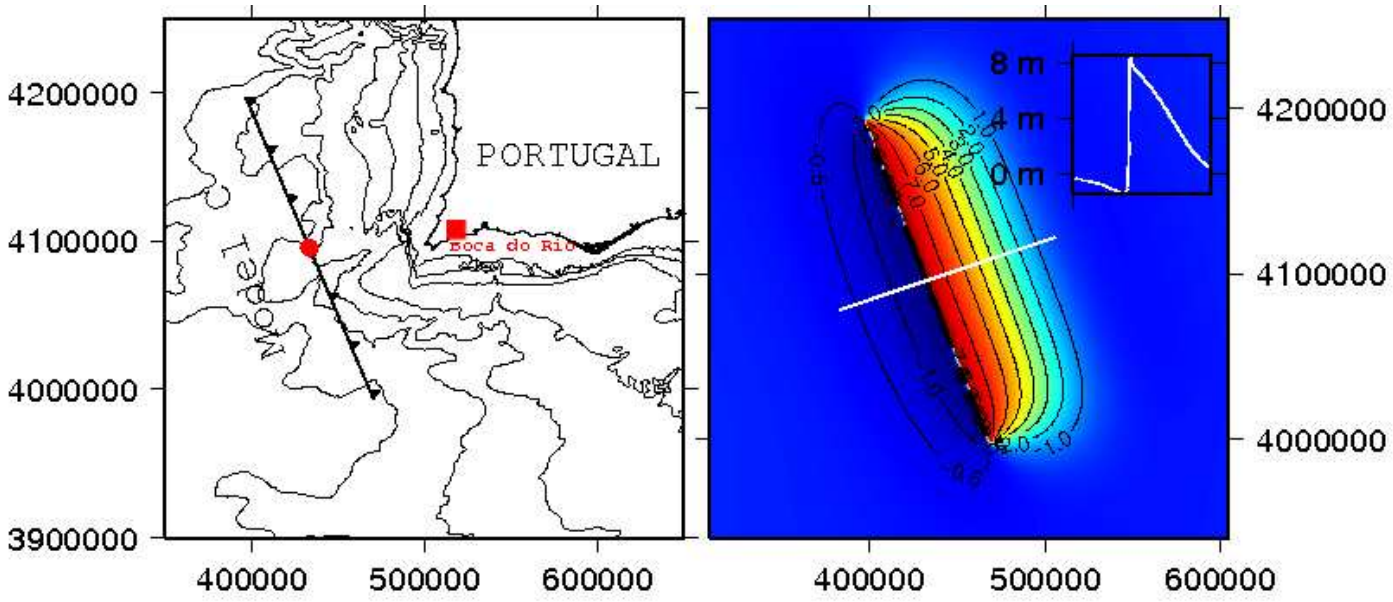

Figure 3.2: *Fault location of the Boca do Rio source model on the left, computed free surface deformation contours with a profile of the initial wave on the right, source parameters in table 3.2.*

The source model used in the work, figure 3.2, is located to the south-west of Sagres in the Gorringe bank area. It is a fault with north-south orientation and other parameters described in table 3.2. In order to obtain the free surface deformation from the modelled earthquake, the analytical expressions for the displacement fields of inclined, finite, dipping, slip faults in the work of Mansinha & Smylie [26] are used through the software Mirone.

Parameter	Value
Fault centre	37.0^o N / 9.75^o W
Length	210 km
Width	75 km
Depth to top	1 km
Strike/Dip/Rake	$340^o/45^o/90^o$
Slip	13.6 m
M_w	8.7

Table 3.2: *Parameters used in the source model for the Boca do Rio test case.*

3.4 Topographic and Bathymetric data

3.4.1 Data sources

This section reviews the data sources of the digital terrain models for both test cases: Boca do Rio and Alvor. We list the several sources used and the corresponding datasets. The digital models prepared cover only the study areas with a high resolution data. Less detailed terrain models for tsunami propagation covering the Gorringe Bank area and the south-west of the Iberian Peninsula were developed by colleagues from the IDL (Instituto Dom Luíz) in Lisbon, also working on the project ERSTA.

The integration and continuity of data between submerged and non submerged areas was the main concern of the grid preparation step. The sources used were:

- **INAG (Instituto da Água):** A digital terrain model with a spatial resolution of 5 m in a stretch of land extending from the shoreline to 200 m inland referenced to Datum 73.

- **IGoE (Instituto Geográfico do Exército):** A digital terrain model covering the Algarve region with a resolution of 8 m was used. The data was referenced to Datum LX with military coordinates.

- **IH (Instituto Hidrográfico):** Two sets of data were used. The first were bathymetric surveys near shore in the Alvor Bay area, obtained by digitizing IH nautical charts. This set is referenced to Datum LX and military coordinates and to the hydrographical zero for the elevation coordinate. The second set were digitized contours offshore of the Algarve region. The available contours are 10, 20, 30, 40, 50, 60, 70, 80, 90, 100, 120, 140, 160, 180, 200, 250, 300, 350, 400, 450, 500, 600, 700, 800, 900 and 1000 m. This set of data is referenced to datum WGS84 and to hydrographical zero.

- **Multibeam survey:** a digital model covering a section between half of the Boca do Rio study area to half of Alvor Bay was available through a collaboration with the NEAREST project [2]. Data coverage ranges from near the shoreline to approximately 100 m in depth and is referenced to Datum WGS84 with a UTM projection.

3.4.2 Grid set-up

COMCOT

For COMCOT we have used a numerical grid system with 3 levels. Figure 3.3 represents the region of the coarser grid, with a spatial resolution of 800 m, the red rectangle is the region of the 2^{nd} level grid, with a resolution of 200 m, and the small black rectangle is the more detailed level with a resolution of 20 m. The first and second level grids were obtained from the IDL colleagues.

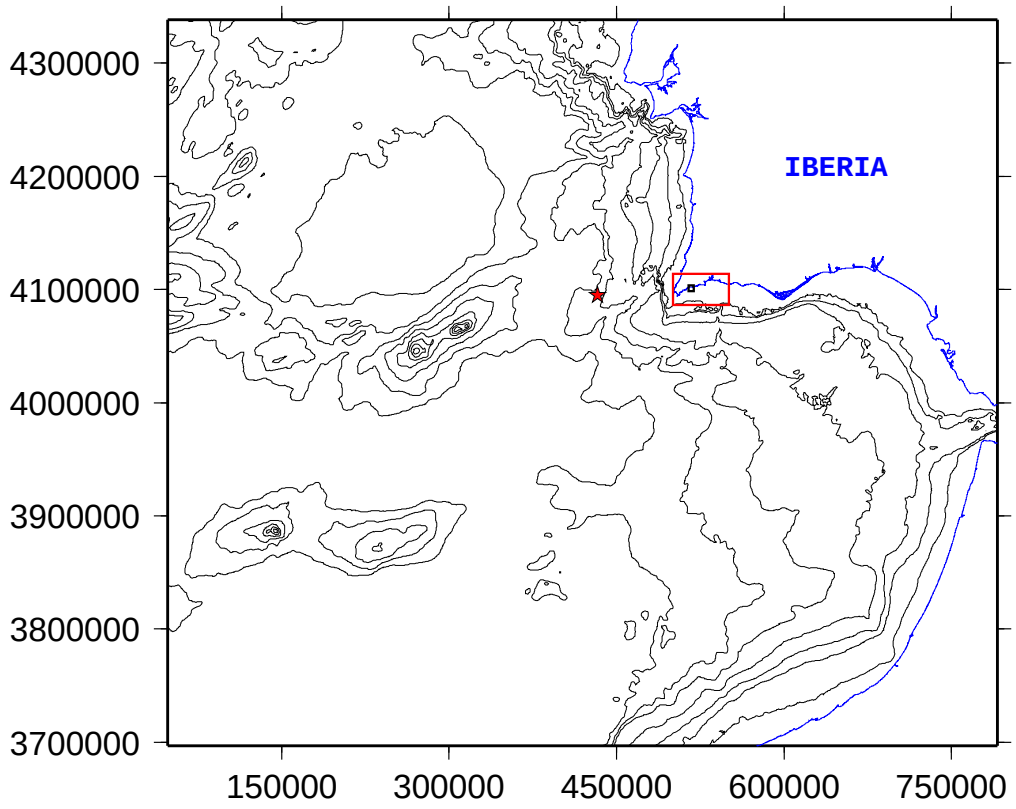

Figure 3.3: *COMCOT grid set-up for the Boca do Rio test case. Figure extents represents the 1^{st} grid level, red rectangle is the 2^{nd} grid level and black rectangle is the 3^{rd} grid level.*

AnuGA

In the AnuGA model the topographic information is represented through a mesh of triangular cells, created by defining its extents and specifying the maximum area for each triangle. To create a digital elevation model for the Boca do Rio test case we have used 2 regions. The first (and coarser) region defines the limits of the terrain model where we have used the extents of the third COMCOT level and a maximum triangle area of 2000 m^2 that means roughly equating to 60 m between each triangle vertex. This region corresponds to the full image of figure 3.4. Inside the latter, a second, more detailed region was defined. It is defined by the red polygon in figure 3.4 where a maximum triangle area of 100 m^2 was used, equating to approximately 15 m between each triangle vertex.

Four boundaries were defined in the mesh (north, east, south and west) and correspond to the

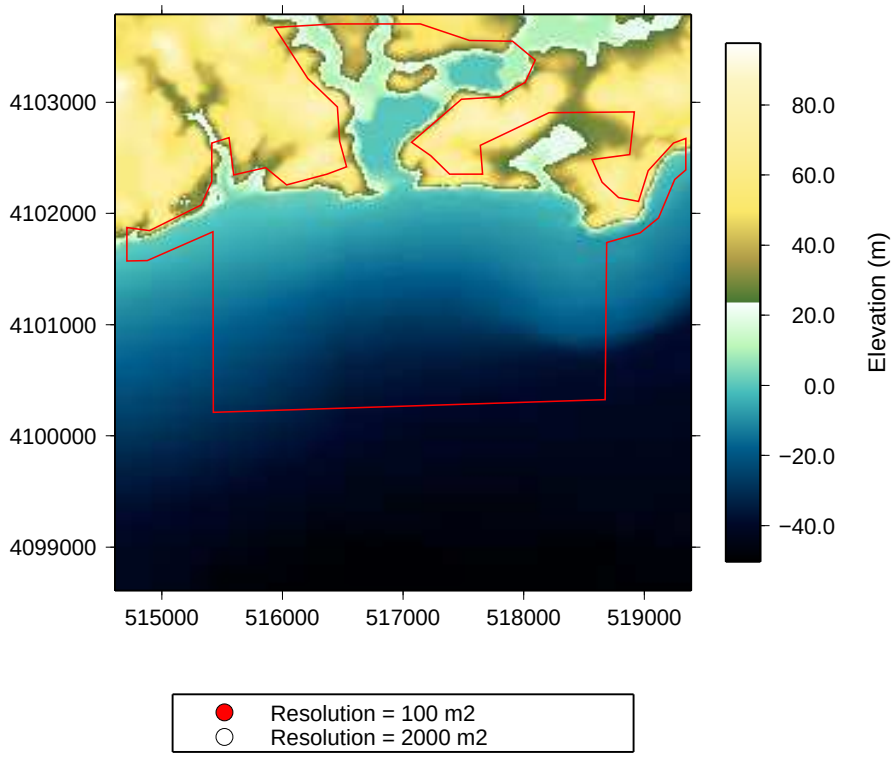

Figure 3.4: *Topography used for mesh generation in AnuGA at Boca do Rio, detailed areas and corresponding triangle areas*

limits of the outer region. The boundary conditions used in the test case were: File boundary condition in the east, south and west boundaries and Transmissive boundary conditition on the north boundary.

Having created the mesh by defining its extents and resolution, the elevation must be added in order to create a digital elevation model (figure 3.5). The elevation information was input in to AnuGA in the format of *xyz* points by converting the third level COMCOT grid into this format using the software GMT [45]. The model uses a penalised least squares technique to attribute an elevation value to the mesh vertices from the input points [30]. Figure 3.5 is a screen capture of the digital terrain model used in the test case.

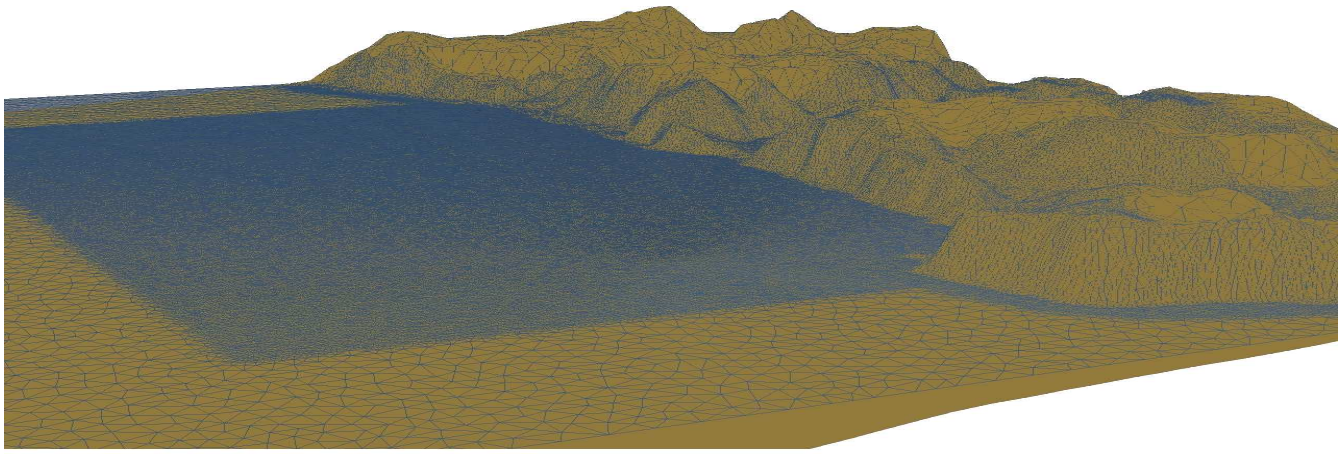

Figure 3.5: *AnuGA grid set-up for the Boca do Rio test case.*

SWAN

The bathymetry and topography in SWAN model is detailed by a single grid. For this test case, the first level grid for COMCOT was used, which is a square grid with a spatial resolution of 800 m.

3.5 Results

This section begins by comparing models COMCOT and SWAN as initial conditions for the AnuGA model. Afterwards, the inundation obtained from both AnuGA configurations and for the configurations of COMCOT using linear or non-linear equations will be evaluated. The evaluation includes the comparison between the models and assessing their similarities with the historical data.

3.5.1 AnuGA input comparison: COMCOT and SWAN

The results described were obtained from wave gauges at the boundaries of the Boca do Rio study area (figure 3.1b).

The runs of both models, COMCOT and SWAN, were executed for a total time of 3000 s and friction was not included. Free surface elevation and momentum were output with an interval of 1 s in SWAN and 10 s in COMCOT.

The AnuGA runs were executed for the same duration and friction was also not included. Elevation and momentum were introduced through the eastern, western and southern boundaries, while the northern boundary was set as transmissive.

West boundary

The water height computed with AnuGA at the western tide gauge is shown in figure 3.6a and compared to the heights computed with AnuGA and COMCOT in figure 3.6b.

AnuGA fed with COMCOT registers a water elevation approximately 50 cm higher than AnuGA input with SWAN. Which on the other hand registers a difference of 1.7 m more on the trough. AnuGA input with SWAN presents more oscillations than the other case.

When comparing the water elevation obtained in AnuGA's and COMCOT's runs at the same gauge, there is a good fit between the waves. The difference in the maximum level is 40 cm. The only exception is the trough, where COMCOT predicts 10 m more than AnuGA with COMCOT input. This might be explained by the difference in the spatial resolutions of the grids. COMCOT's wave was obtained on a grid with 800 m resolution while the resolution in AnuGA is approximately

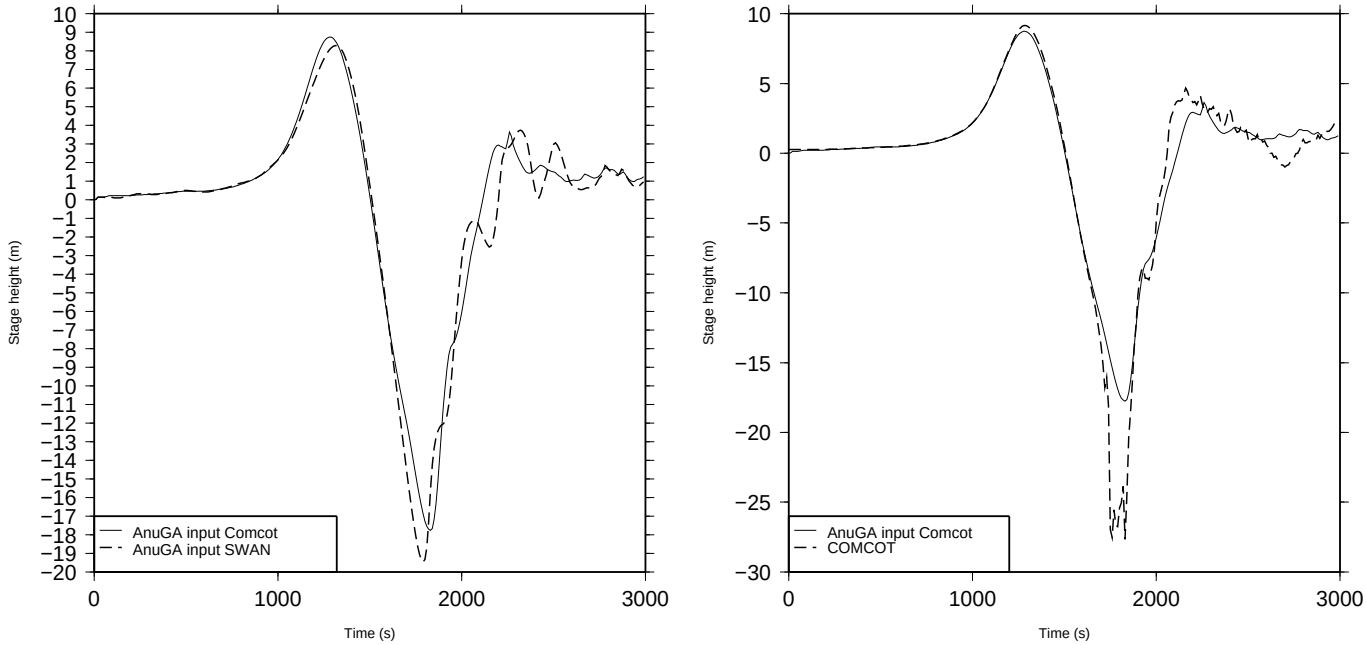

(a) (b)

Figure 3.6: *West boundary tide gauges elevation comparison. (a) Obtained in AnuGA's runs input with COMCOT and SWAN. (b) Obtained in AnuGA's run and COMCOT's run.*

60 m at the gauge location.

South boundary

Figure 3.7 shows the water levels at the south boundary tide gauge from AnuGA with COMCOT and SWAN input.

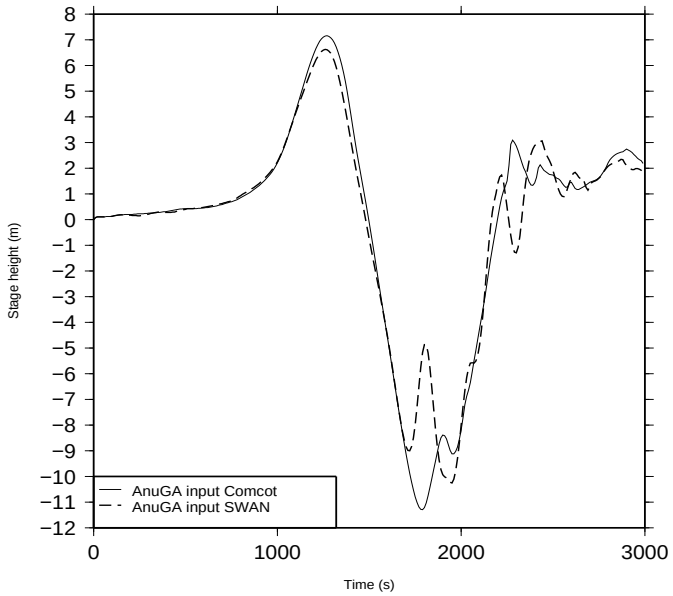

Figure 3.7: *South boundary tide gauge water levels from AnuGA with COMCOT and SWAN input.*

At the southern gauge, the fit between both waves is good, although AnuGA input with SWAN presents more high frequency oscillations than AnuGA input with COMCOT. The difference in the maximum water level is about 0.5 m.

East boundary

The results obtained at the eastern boundary gauge are similar to those obtained at the other boundaries. AnuGA input with SWAN also presents high frequency oscillations in water levels that are not so noticeable in the AnuGA input with COMCOT.

3.5.2 Inundation: AnuGA and COMCOT

Figure 3.9a shows the gauges located at the 5 m isobath and indicates the location of gauge #6 for which the results 3.9b and 3.9c are plotted.

The analysis of the propagation results for each of the configurations used was performed using gauge #6 at the 5 m isobath. Comparison of both AnuGA configurations does not show significant differences. For COMCOT, even though the linear configuration presents much more noise than the non-linear one, on average the waves are not significantly different.

A cross shore profile was drawn to analyse the inundation. The following figure presents the inundation height extracted from the modelled maximum water levels.

Except for COMCOT with linear equations, in all tested cases the water levels decrease on land

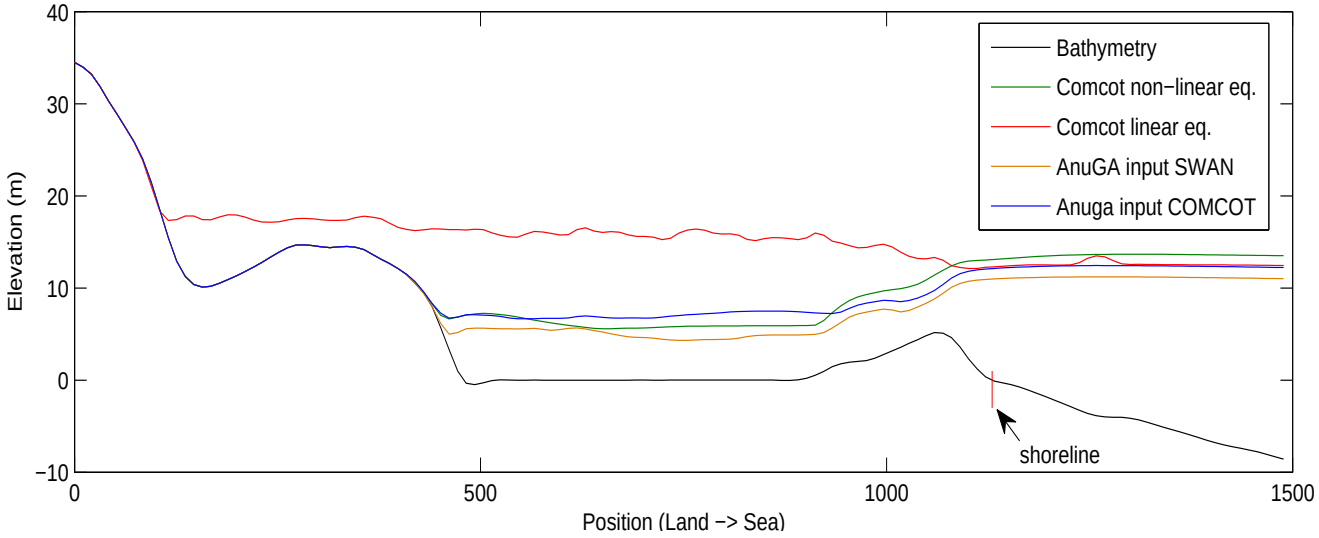

Figure 3.8: *Cross shore inundation profile at Boca do Rio. See figure 3.9a for prolife location.*

in relation to the water level above the 5 m isobath. Table 3.3 summarizes the inundation results for each of the tested cases.

It was not possible to analyse the cause for COMCOT's linear configuration behaviour since this option is not documented. In the next section we compare each set of results with the historical data.

Source	max. *run-up* (m)	max. *run-in* (m)
AnuGA input with COMCOT	12.6	839.7
AnuGA input with SWAN	11.4	836.9
COMCOT linear eqs.	20.6	1558.2
COMCOT non-linear eqs.	14.4	836.9

Table 3.3: *Summary of the modelled inundation results with the four configurations.*

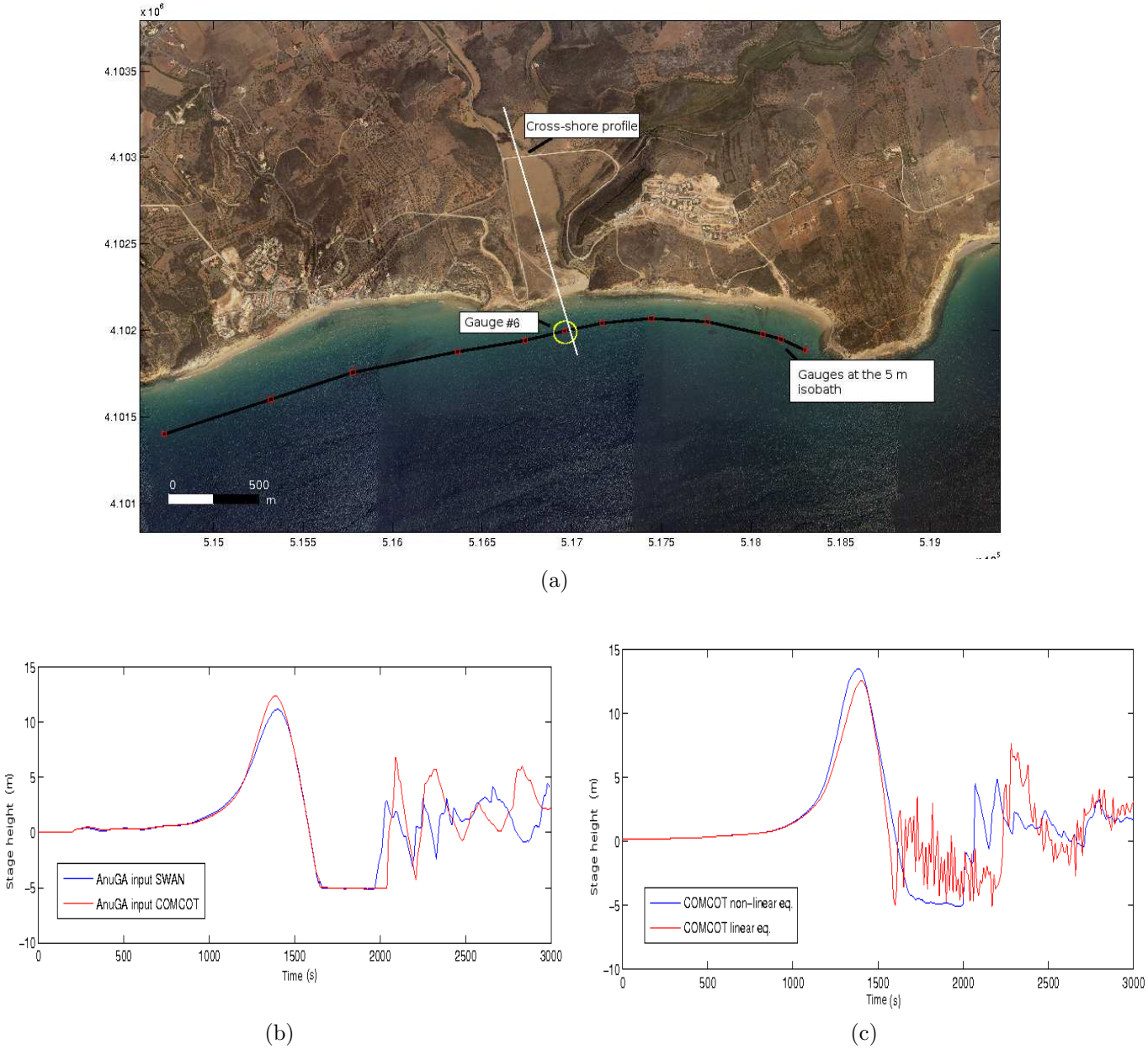

Figure 3.9: *(a) Aerial photograph showing gauge and profile location at Boca do Rio study area. (source: IPCC/DGRF 2005). (b) AnuGA water levels at gauge #6 (c) COMCOT water levels at gauge #6.*

3.5.3 Comparison with historical data

Table 3.4 summarizes the historical data available at the test site and a comparison can be made with the modelled results in table 3.3. The results achieved with the linear equation configuration in COMCOT seem to overestimate the *run-up* , since the wave height at the 5 m isobath is similar in all the cases but the *run-up* is high when compared to the others.

Source	max. *run-up* (m)	max. *run-in* (m)
Data from historical reports	11 a 13	2500
Tsunami sedimentary layer	-	980

Table 3.4: *Summary of the data obtained from historical reports.*

When comparing the modelled *run-in* results, all the configurations underestimate the historical data. Nevertheless, care must be taken since the historical data is based on observations and can be exaggerated and also the topography used to model this event does not necessarily match the topography of the historical data.

Figure 3.10 shows the inundation extents of the modelled cases with the tsunami sedimentary layer identified by Hindson & Andrade (1999) [16] at Boca do Rio.

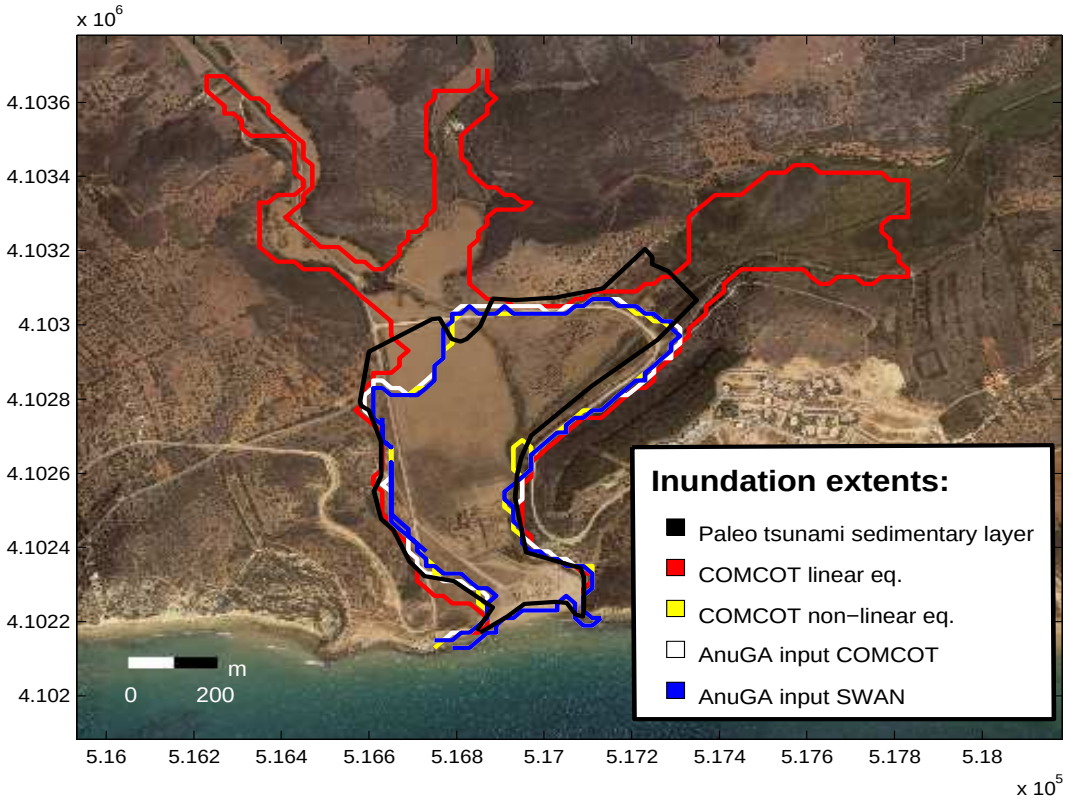

Figure 3.10: *Comparison of the modelled inundation extents with the tsunami sedimentary layer extents at Boca do Rio.*

Chapter 4

Alvor test case

The aim of the Alvor test case is to intensively test the inundation capabilities of numerical models AnuGA and COMCOT.

We used 81 fault models obtained from varying fault parameters: dip and depth. The first is used in a range between 20 and 60^o, with a 5^o step, and the second between 0.5 and 50.5 km, with a step of 5 km until 30.5 km and 10 km from then on. The fault models were used to create the initial conditions that input numerical models COMCOT and SWAN. At this test case we have only used some of the configurations tested at Boca do Rio. For the COMCOT set-up, a numerical scheme with 4 levels of grid resolution was used along with non-linear equation configuration without friction for the inundation modelling. For the AnuGA set-up, initial conditions were imposed from the output of the SWAN model. This option has proven to be less time consuming and has not exhibited significant differences from using COMCOT. Nevertheless, comparison of both inputs was made in the case of highest *run-up* by AnuGA. To fulfil the purpose of this test case, extensive comparisons were made of the inundation parameters *run-up*, *run-in* and amplification factor derived from both models results.

Taking advantage of a multibeam bathymetric dataset, we also tested the effect of using this dataset against a bathymetric dataset based on digitized nautical charts.

This chapter starts by describing the Alvor test site and the surrounding environment. This is folowed by an overview of the fault models used for the test case and the datasets used for creating the topographic and bathymetric elevation models for the runs. Finally we present the results and evaluate them according to the research objectives.

4.1 Site description

The area surrounding the coastal city of Alvor (figure 4.1) was chosen for intensive testing of the numerical models. One of the reasons for this choice is the availability and quality of the topographic and bathymetric data available. An evaluation of these data will be made in section 4.3. Another reason for this choice is the variety of morphological environments present in this coastal area. In general the study area is a bayed beach limited on the west by an artificial inlet and an important headland. In the centre of the bay there is another inlet altered by human intervention to allow navigation in and out of the coastal lagoon, "Ria de Alvor". The eastern part of the bay is

constrained by a small headland. In this area there is intense human occupation near the beach at Torralta, mainly a tourist resort, and further inland near the town of Alvor, delimited by the white polygon in figure 4.1a.

We have divided the study area into three zones as detailed in figure 4.1b.

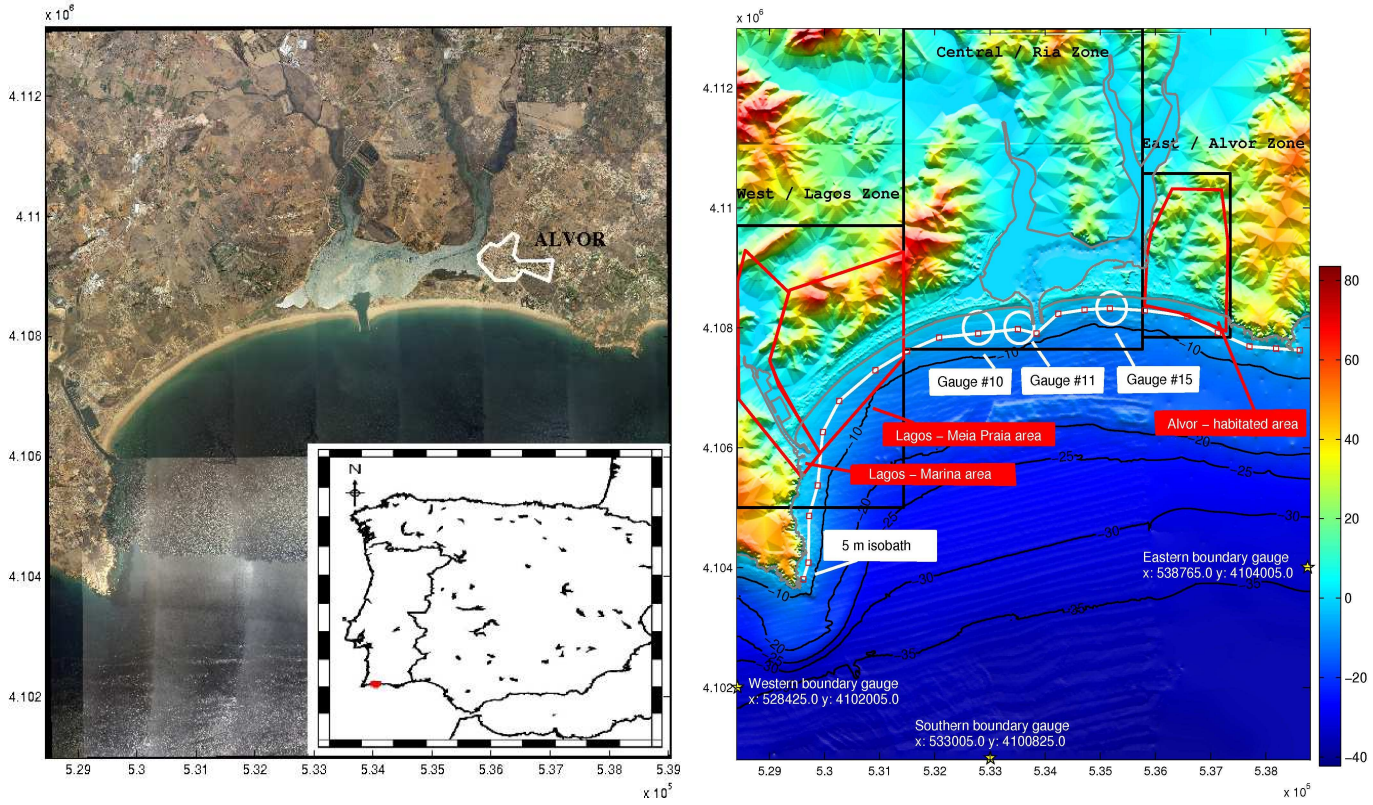

(a) (b)

Figure 4.1: *(a) Aerial photograph of the Alvor study area (source: IPCC/DGRF 2005). (b) Grid image of the study area with location of the wave gauges on the boundaries and the 5 m isobath, extents of the analysis zone of Alvor.*

4.2 Source models

The location of the fault used in the source models for the Alvor test case was obtained from a collaboration with project TRANSFER (Tsunami Risk ANd Stratagies For European Region) [5]. This project aims to attain a better knowledge of the vulnerability, danger and risk of tsunamis in the Euro-Mediterranean region and to study strategies for minimizing the risk.

Since only the information of the fault location and orientation was available, we have chosen to use the parameters of a fault described in Richardson *et. al.* (2006)[33] to create a source model.

To achieve the extensive testing of models COMCOT and AnuGA, a range of source parameters were used in order to account the differences in inundation parameters: *run-up* and *run-in* . The 81 source models were obtained by using a range of dip angles and varying the fault depth. The dip angle interval is defined between 20 and 60° in 5° steps and the source fault depth is defined between

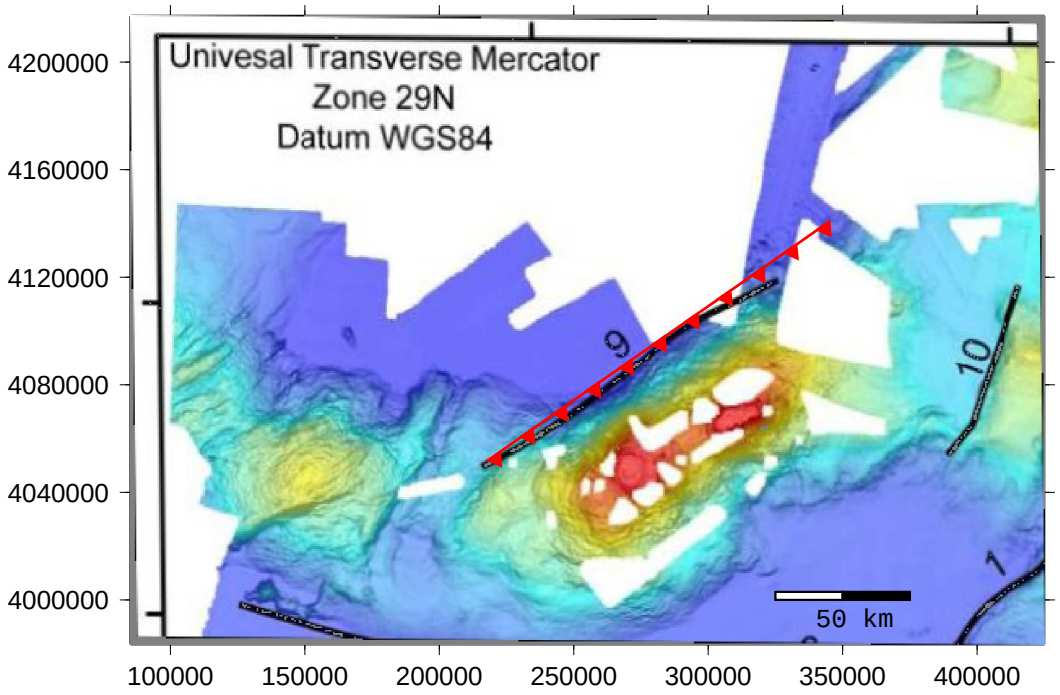

Figure 4.2: *Fault 9, in black the fault output of TRANSFER project; in red, the fault used for the source models in Alvor's test case. (adapted from TRANSFER project)*

0.5 and 50.5 km with 2 different steps: the first of 5 km - between 0.5 and 30.5 km, and the second 10 km - between 30.5 and 50.5 km. Table 4.1 summarizes the source model parameters and their values.

Parameter	Value
Length	150 km
Width	75 km
Strike	55°
Depth	0.5 to 50.5 km
Dip	20 to 60°
Slip	13.6 m
M_w	8.4

Table 4.1: *Source model parameters used in Alvor test case.*

The free surface elevation for each of the source models was produced in the software Mirone using the method proposed by Mansinha & Smylie [26].

4.3 Topographic and Bathymetric data

4.3.1 Data sources

The data sources used for the creation of Alvor's digital terrain model are described in section 3.4.1. The same data sets were used for both test cases. This was possible since the datasets of INAG, IGoE and IH cover all the Algarve region and the multibeam survey covers part of the Alvor and Boca do Rio study area. This section will be used to describe the procedure used.

The first task was to convert the data into a common reference system. Datum WGS84 was chosen with the UTM zone 29N projection and reference to the mean sea level for ther vertical coordinate. For topographic data, INAG data was fully used and complemented with data from IGoE military charts. For bathymetric data, the multibeam survey was used where possible and complemented with IH surveys data and digitized contours.

For the Alvor, two grid levels were created with resolutions of 50 m and 10 m, respectively. Figure 4.3 shows the 10 m terrain model of Alvor, identifying the sources used and theie respective coverage.

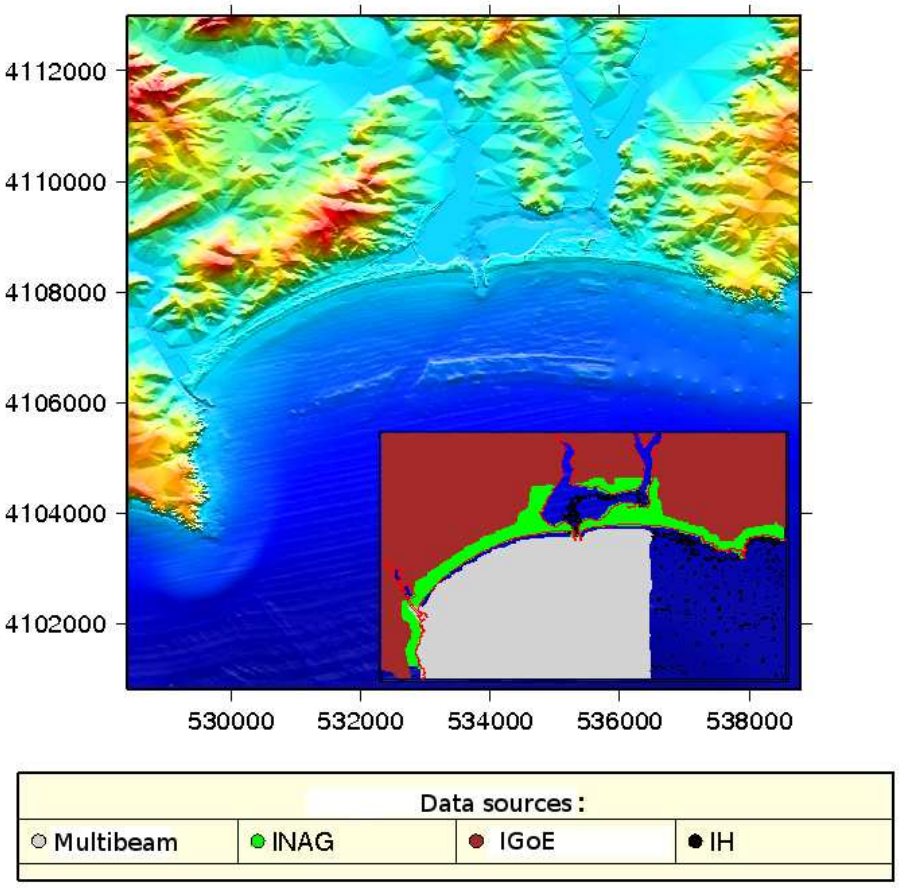

Figure 4.3: *Overview of the Alvor study area data sources and respective coverage (colours: Grey - Multibeam data; Green - INAG data; Red - IGoE data; Black - IH data).*

4.3.2 Grid set-up

COMCOT

For the COMCOT set-up, a numerical scheme with 4 levels of grid resolutions was used. The first two level grids were obtained from IDL.

Figure 4.4 puts the grid coupling used in model COMCOT into a spatial context. The levels have an increasing spatial resolution. The first level with an 800 m resolution, is used for propagation between the source and the continental shelf; the second level with a 200 m resolution, is used for the propagation on the continental shelf. The third and fourth level have a 50 and 10 m resolution and cover the propagation at the entrance of the study area and the 10 m grid aims to provide maximum detail to the inundation area.

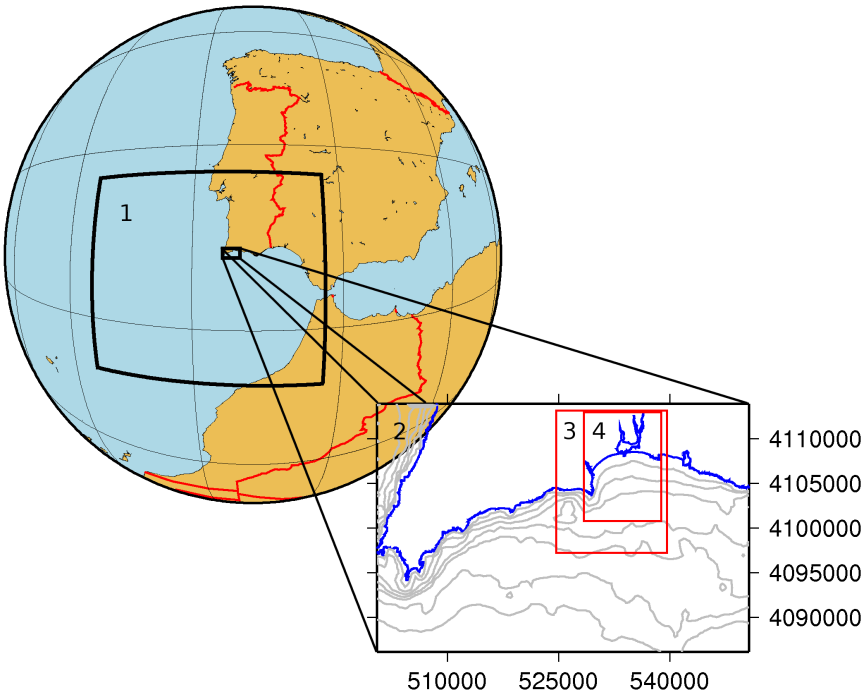

Figure 4.4: *Alvor grid coupling for the COMCOT model.*

AnuGA

The same process as described for Boca do Rio in section 3.4.2 was used to create the digital model for AnuGA.

For creating the elevation model, besides the wider region, three regions of detail were used (figure 4.5). For the broad area that defines the extents of the terrain model, a maximum triangle area of 10000 m^2 was used. A less coarser region was defined in the submerged near-shore area (red polygon in figure 4.5) to enhance detail between the 15 m isobath and the shoreline. For this a maximum triangle area of 2500 m^2 was used, corresponding to about 70 m between each triangle vertex. To detail the inundation area (black polygon in figure 4.5) a maximum triangle area of

100 m^2 was used, which roughly represents a distance of 15 m between each triangle vertex. An area near the western branch of the "Ria de Alvor" (blue polygon in figure 4.5), where inundation is not expected but can occur in extreme cases, was detailed with a maximum triangle area of 500 m^2.

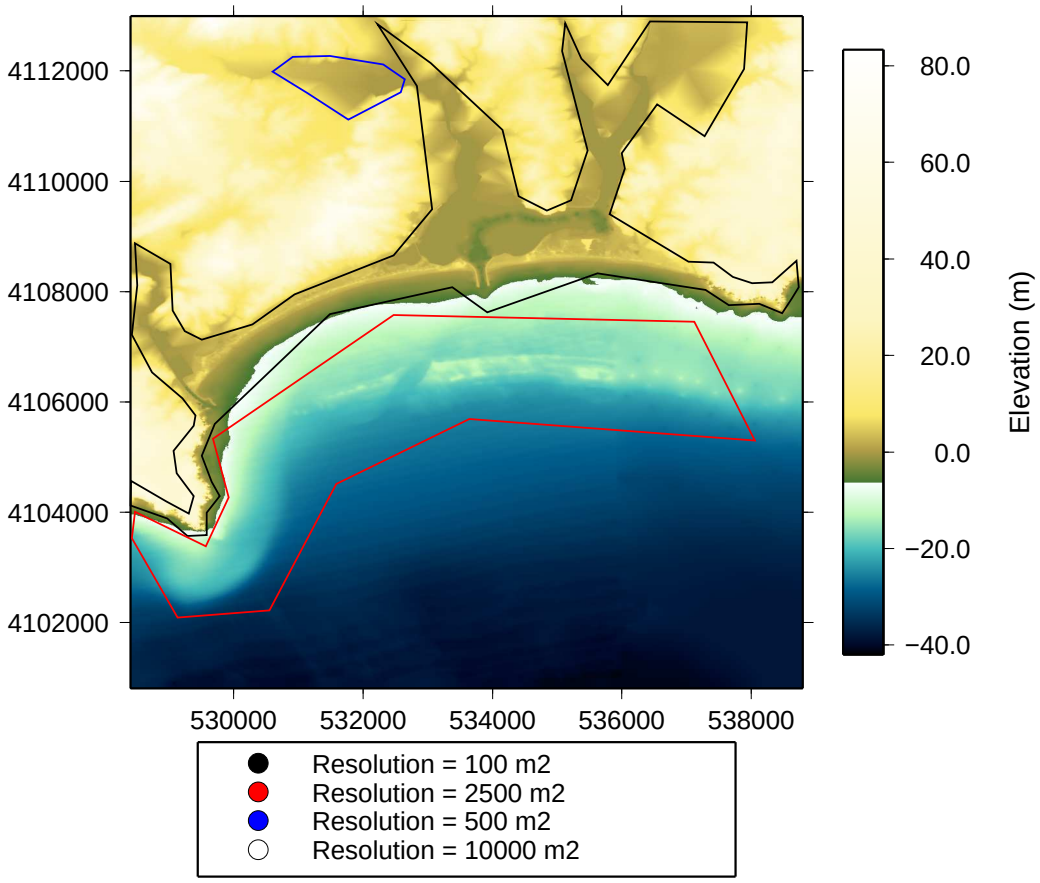

Figure 4.5: *Identification of the detailed regions and resolution used to create the AnuGA's digital terrain model at the Alvor study area.*

SWAN

The grid level 1 of COMCOT was used for the SWAN model. It corresponds to the level grid with a resolution of 800 m.

4.4 Results

In this section we present and evaluate the modelled results. First a comparison of AnuGA input with COMCOT or SWAN for a selected fault model is made. We then make an evaluation of the effect on wave propagation of using datasets with different resolution for the creation of the bathymetric grid. Finally, we present an extensive comparison of the inundation parameters of *run-up*, *run-in* and amplification factors for the 81 fault models created.

Figure 4.6 shows the location of the gauges at the boundaries of the Alvor study area, the location of the gauges at the 5 m contour line and the zones and areas on land for the results analysis.

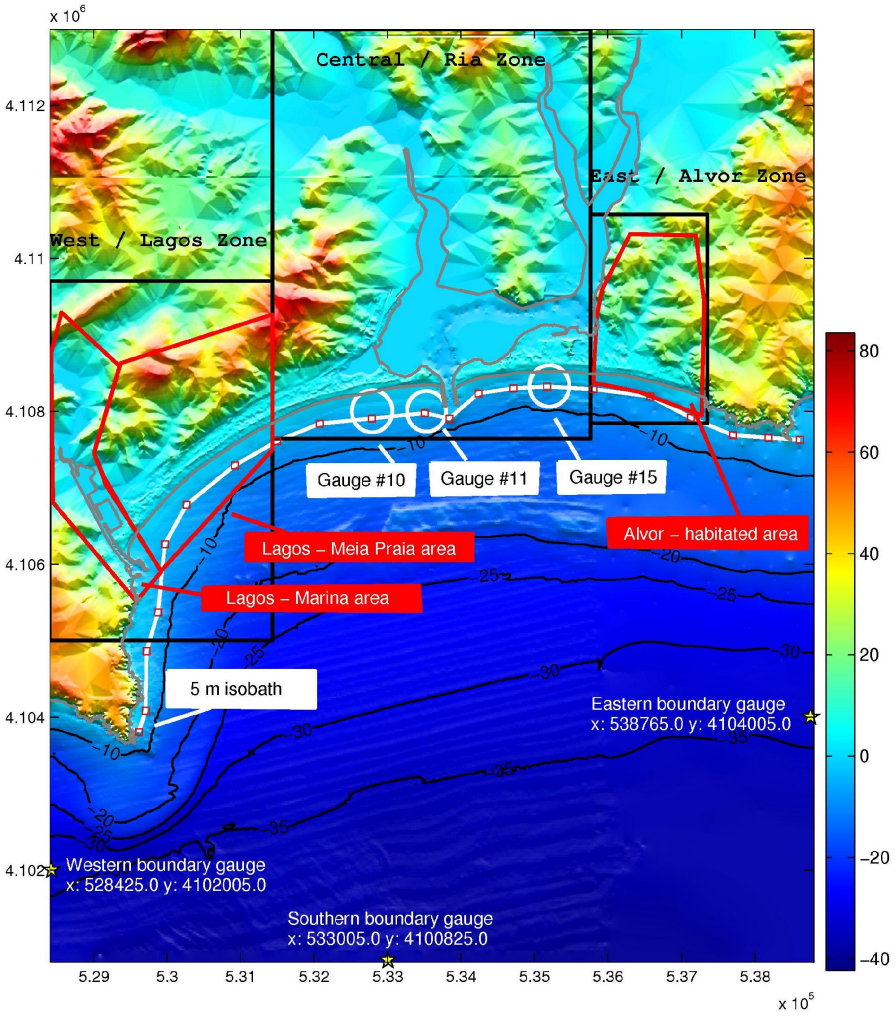

Figure 4.6: *Grid image of the study area with location of wave gauges on the boundaries and at the 5 m contour line; delimitation of inland zones used in the analysis .*

4.4.1 AnuGA input comparison: COMCOT and SWAN

The results presented in this section were obtained with source model parameters of a dip angle of 35° and fault depth of 25.5 km. This source configuration was chosen since, as we will show later, resulted in the highest *run-up* and *run-in* values modelled by AnuGA input with SWAN.

The COMCOT and SWAN model runs were carried for a total time of 4500 s with no friction included. The results presented were obtained at the boundaries and at the 5 m isobath gauges (see figure 4.6 for location reference).

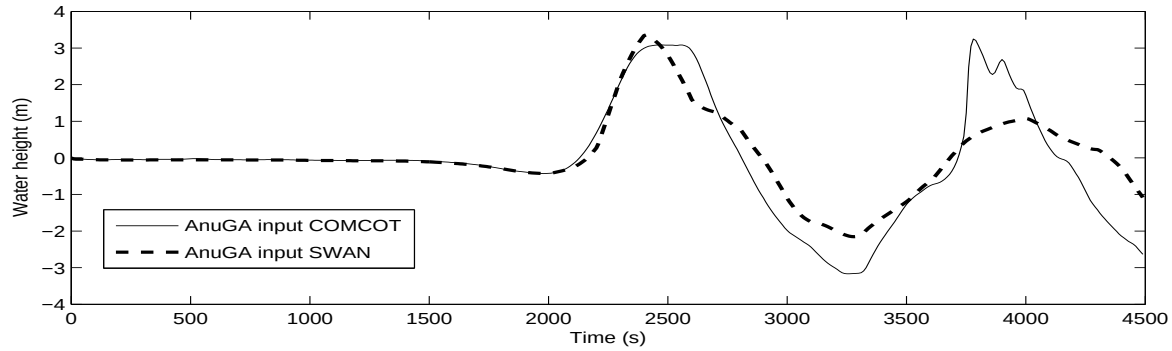

Figure 4.7: *Wave gauge record at the western boundary in Alvor test site. (for location see figure 4.6)*

West boundary

The gauge record shows that the modelled first wave is similar in AnuGA with both input. The second wave's behaviour is different, here AnuGA input with COMCOT registers a wave 2 m higher than with SWAN, which is a difference of about 60 %. Nevertheless, the significant difference in the second wave is not reflected near the shoreline, as is demonstrated later when the analysis of the wave at the 5 m contour line is made.

South boundary

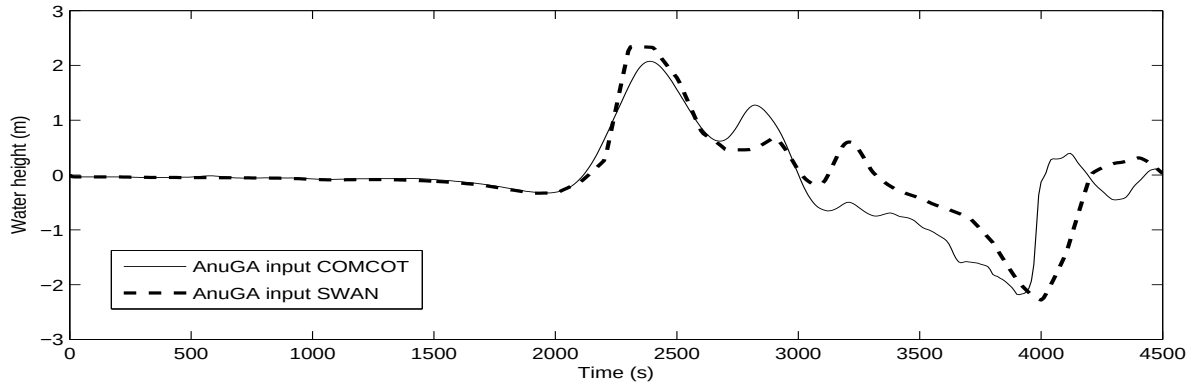

Figure 4.8: *Wave gauge record at the southern boundary in Alvor test site. (for location see figure 4.6)*

The wave gauge record at the southern boundary does not exhibit significant differences in amplitude between the different sources but indicates that the waves are slightly out of phase. The second wave of AnuGA input with COMCOT is registered before than the wave from AnuGA input with SWAN.

East boundary

The wave record at the eastern boundary shows the same trend as the southern boundary one.

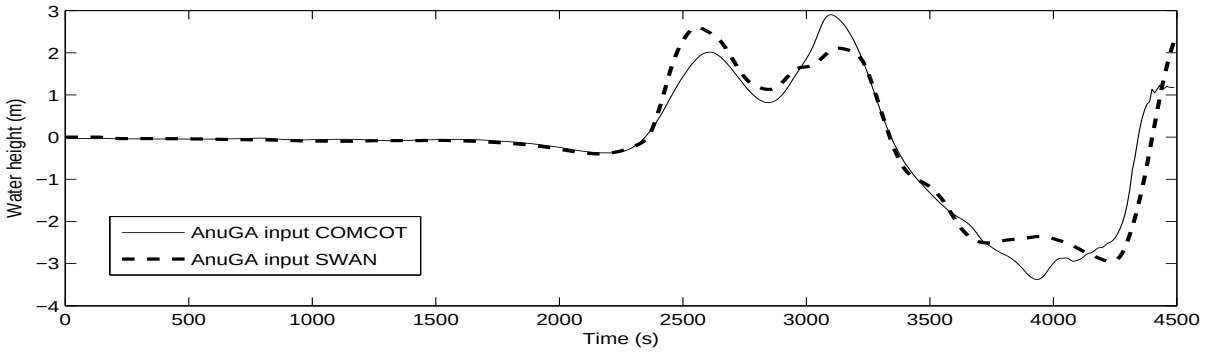

Figure 4.9: *Wave gauge record at the eastern boundary in Alvor test site. (for location see figure 4.6)*

Wave form at the 5 m isobath

Figure 4.10 shows the wave forms captured by gauges #10 and #15 at the 5 m isobath (see figure 4.6 for location).

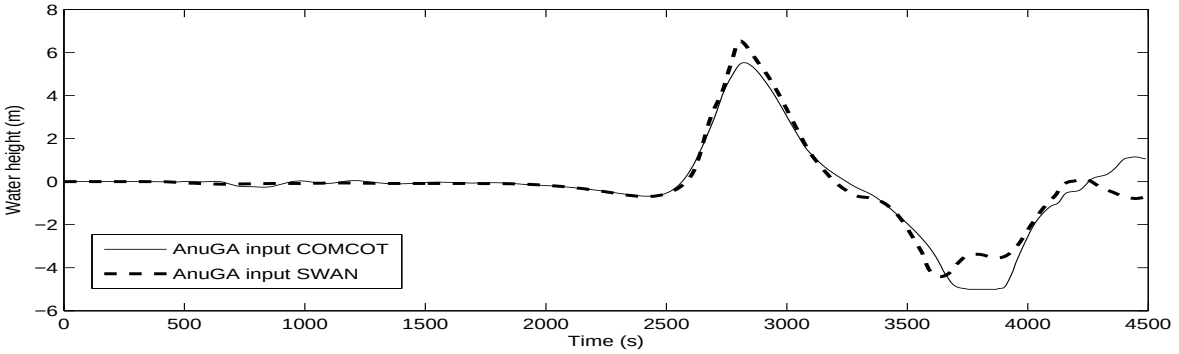

(a)

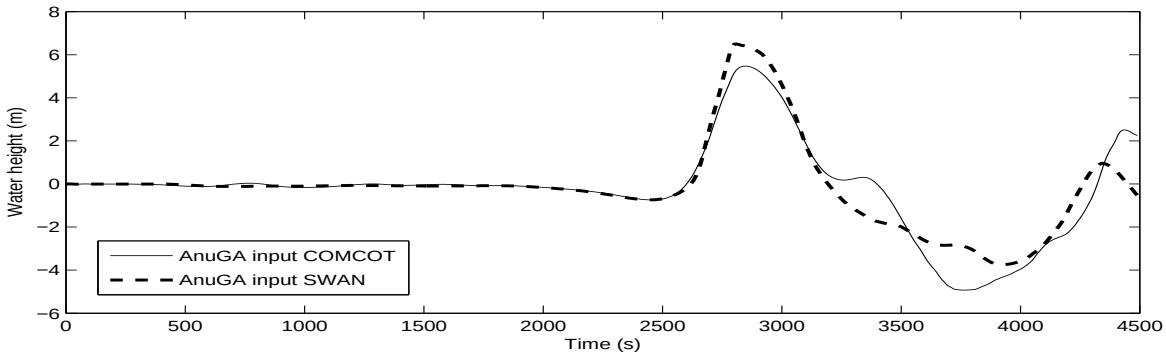

(b)

Figure 4.10: *Wave gauges at the 5 m isobath. (a) Gauge #10. (b) Gauge #15. (see figure 4.6 for location).*

There are only minor differences between the different waves at the 5 m isobath. The differences range from a maximum of 15 % to a minimum of 9 % in several wave sections. Moreover, the significant differences on the second wave registered on the western boundary are not significant near the shoreline, since a 60 % difference has diminished to a 15 % difference.

4.4.2 Multibeam bathymetry usage

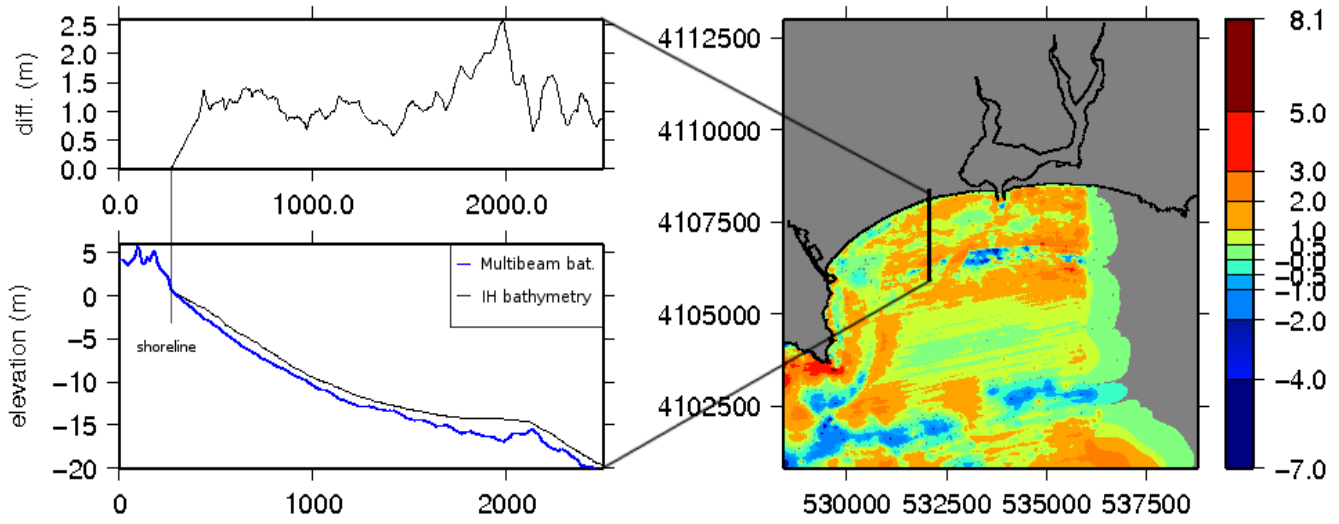

Figure 4.11: *On the left, the top figure is a plot of the difference on the elevation of the grids in meters; the bottom figure is a plot of the elevation obtained from the IH (in black) and Multibeam (in blue) bathymetric grids in the profile. On the right, Colour composition of the multibeam and IH bathymetry grid differences.*

In this test case we used two different bathymetric data sets to calculate the bathymetry grids. The first grid, identified as multibeam bathymetry, is composed multibeam survey data and complemented with IH digitized data where multibeam was not available. The second grid, identified as IH bathymetry, is composed of IH digitized data only. Both grids were interpolated into a spatial resolution of 10 m. Figure 4.11 shows the difference between the IH bathymetry and the multibeam bathymetry.

Analysis of propagation was done for each model separately. We compared the differences of the wave forms at the entrance of the study area using the gauges on the boundaries and the differences at the 5 m contour line using gauge #11 (see figure 4.6).

AnuGA

Three runs were performed in this test case. In all of them AnuGA was fed with SWAN. Table 4.2 summarizes the maximum water heights at the western and southern boundary gauges and at the 5 m isobath gauges.

The table indicates that the differences between the wave of IH and multibeam bathymetry at the boundaries are minimal and that, even though they have augmented to the 5 m isobath, they continue to be insignificant. The wave forms of the run with fault parameters of 30^o dip and 5.5 km depth are shown in figure 4.12.

		IH Bathymetry			Multibeam Bathymetry		
		Boundaries			Boundaries		
Dip (^{o})	Fault depth (km)	West (m)	South (m)	5 m isobath (m)	West (m)	South (m)	5 m isobath (m)
30	5.5	2.38	2.18	5.69	2.38	2.15	5.51
35	25.5	3.38	2.38	6.77	3.36	2.35	6.53
60	50.5	1.86	1.45	3.58	1.85	1.45	3.88

Table 4.2: *AnuGA maximum water heights at the boundary and 5 m isobath gauges.*

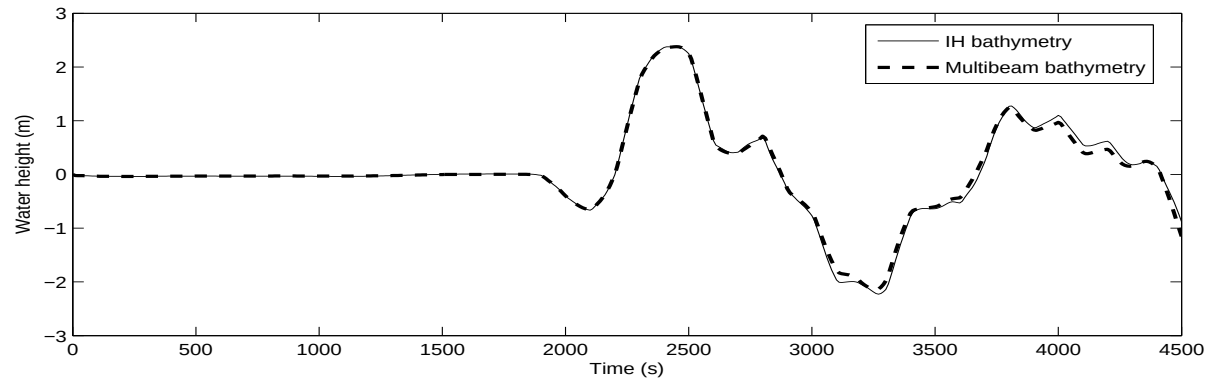

(a)

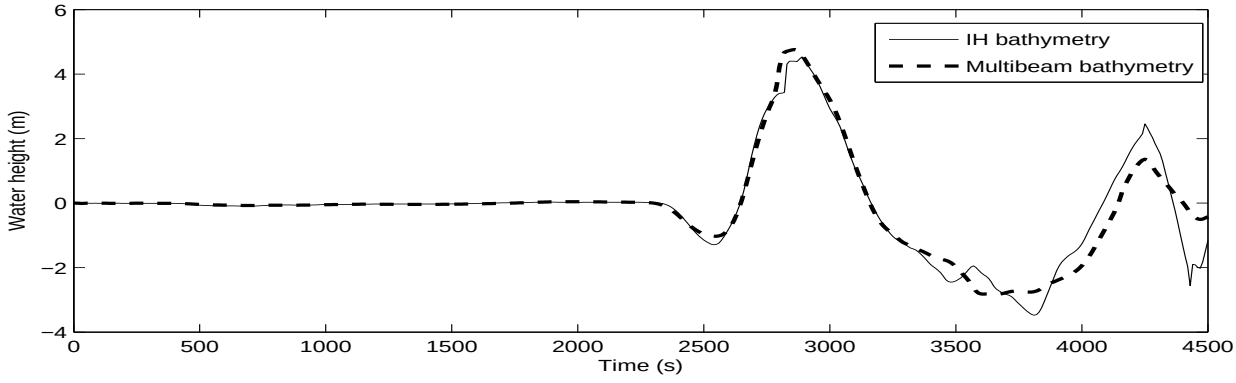

(b)

Figure 4.12: *Comparison of wave forms for a run with fault parameters of 30º dip and 5.5 km depth. (a) Western boundary gauge. (b) Gauge #11 at the 5 m isobath. (Gauge location on figure 4.6).*

COMCOT

For the COMCOT runs, the same source models were used as described before. Table 4.3 summarizes the maximum water heights at the western and southern boundaries and at the 5 m isobath gauges.

		IH bathymetry			Multibeam bathymetry		
		Boundaries			Boundaries		
Dip (^{o})	Fault depth (km)	West (m)	South (m)	5 m isobath (m)	West (m)	South (m)	5 m isobath (m)
30	5.5	5.00	3.02	7.17	4.77	2.97	7.02
35	25.5	4.38	2.22	7.50	4.48	3.16	6.74
60	50.5	2.59	1.57	6.18	2.43	1.56	6.09

Table 4.3: *COMCOT maximum water heights at the boundaries and 5 m isobath gauges.*

Although it was not possible to have exactly the same wave at the fourth level grid entrance, the differences are not significant. Except at the southern boundary gauge for a run with dip 35° and depth of 25.5 km, where difference is approximately 1 m. Nevertheless, analysis of the wave at the 5 m isobath in figure 4.13 shows no major differences.

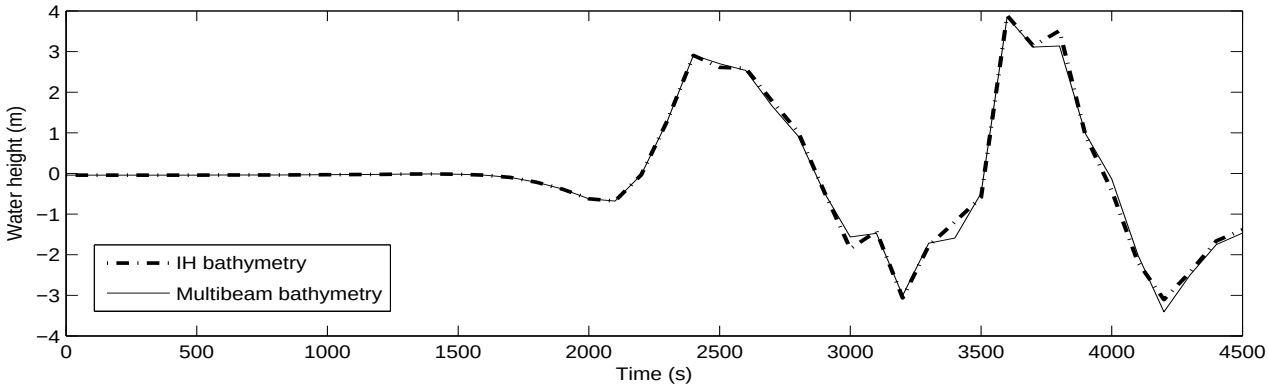

(a)

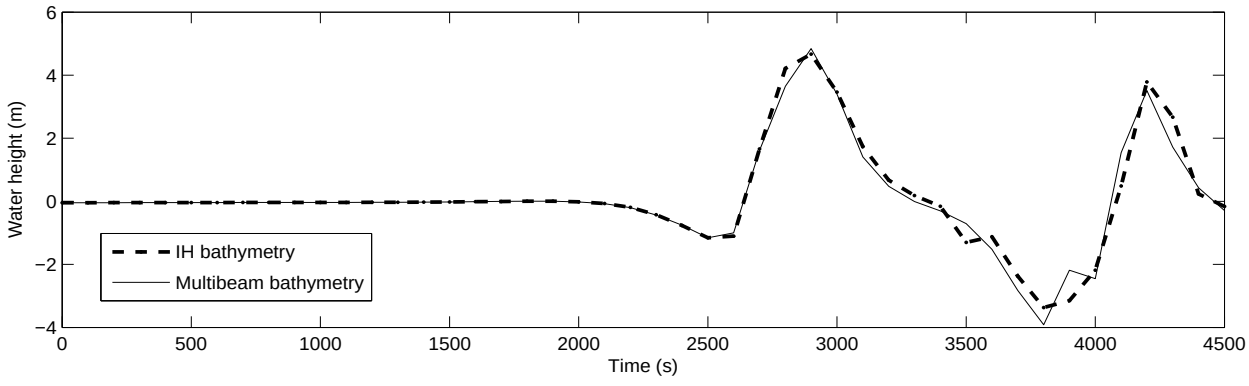

(b)

Figure 4.13: *Comparison of wave forms for run with parameters dip 30º and depth 5.5 km. (a) Western boundary gauge. (b) Gauge #11 at the 5 m isobath. (Gauge location on figure 4.6).*

4.4.3 Inundation modelling results

In order to account for the environment and spatial location of the results, we have divided the following analysis in three different zones (figure 4.6).

The West/Lagos zone covers an area from Cape Ponta da Piedade on the western part of the study area to half of Meia-Praia beach which is an area potentially sheltered to a waves approaching from the south-west. The Central/Ria zone covers a coastal lagoon environment, which is a lowlying area in direct connection with the ocean through the Alvor inlet. In this zone the *run-in* is expected to be larger than in the other zones. The East/Alvor zone covers the eastern part of the study area from half of Alvor beach to the cliffs on the eastern tip. This zone encloses the villages of Alvor and Torralta which lie close to the shoreline. Within this zone we expect to analyse possible impacts on inhabited areas.

We start by analysing the *run-up* results. Here we look for the highest value in each zone and the evolution from zone to zone. At the end of the following section we present two inundation maps obtained from the runs with the highest *run-up* for both models. The following section analyses the *run-in* in four different environments. At the end we present two inundation maps obtained from the runs with the highest *run-in* for both models. The final section compares the amplification factor obtained from the relationship between maximum water height at the source and the maximum water height at the beach, i.e. at the 5 m isobath.

Run-up

The maximum height range obtained from each model is different and, while it was not possible to use the same colour scale, the same scale was used for each model. Maximum water heights range from 3 to 14 m in COMCOT and from 2.5 and 6.5 m in AnuGA.

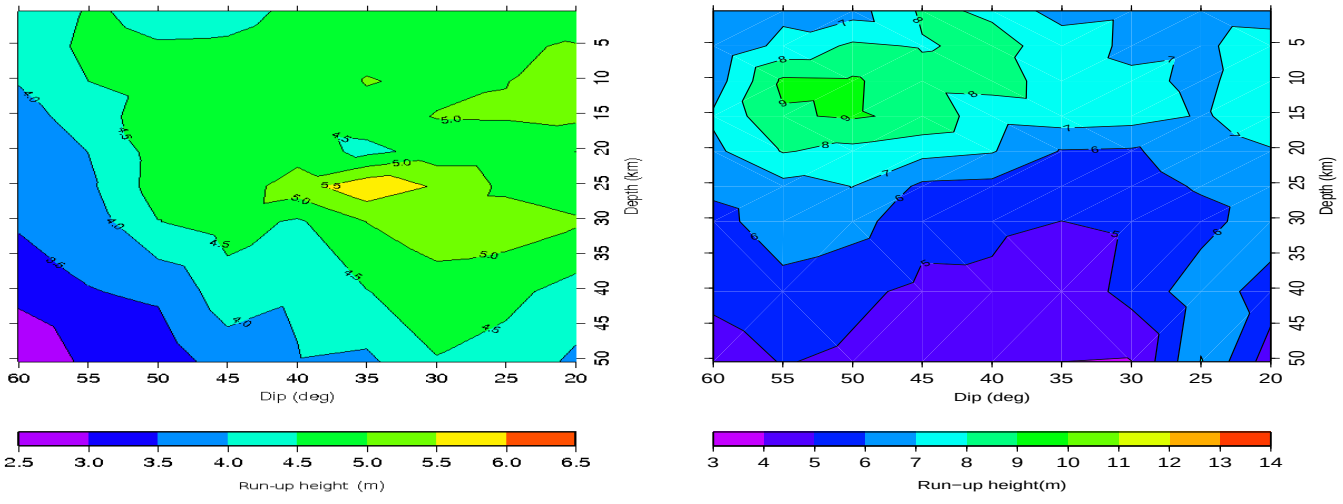

(a) (b)

Figure 4.14: *Run-up at the West/Lagos zone. (a) AnuGA e (b) COMCOT. In this figure we plot contours of the maximum water height at the West/Lagos zone in function of source parameters: dip on the horizontal axis and depth on the vertical axis. (see figure 4.6 for zone bounds).*

Figure 4.14 shows the *run-up* results at the West/Lagos zone. Model AnuGA maximum heights range from 5 to 6 m and occur with the fault models of smaller dip angle (between 30 and 35°) and intermediate fault depth (between 25 and 35 km). For greater depths the variation of the dip angle is an important factor controlling the *run-up*, with the lowest values being attained at the highest dip angle and deepest fault. The COMCOT model is more sensitive to variations in the fault depth. Maximum values occur at shallower depths (5 to 15 km) and highest dip angle (50 to 55°). An exception is the source model with dip angle of 25°, where the *run-up* is virtually constant at all depths: from 6 to 7 m.

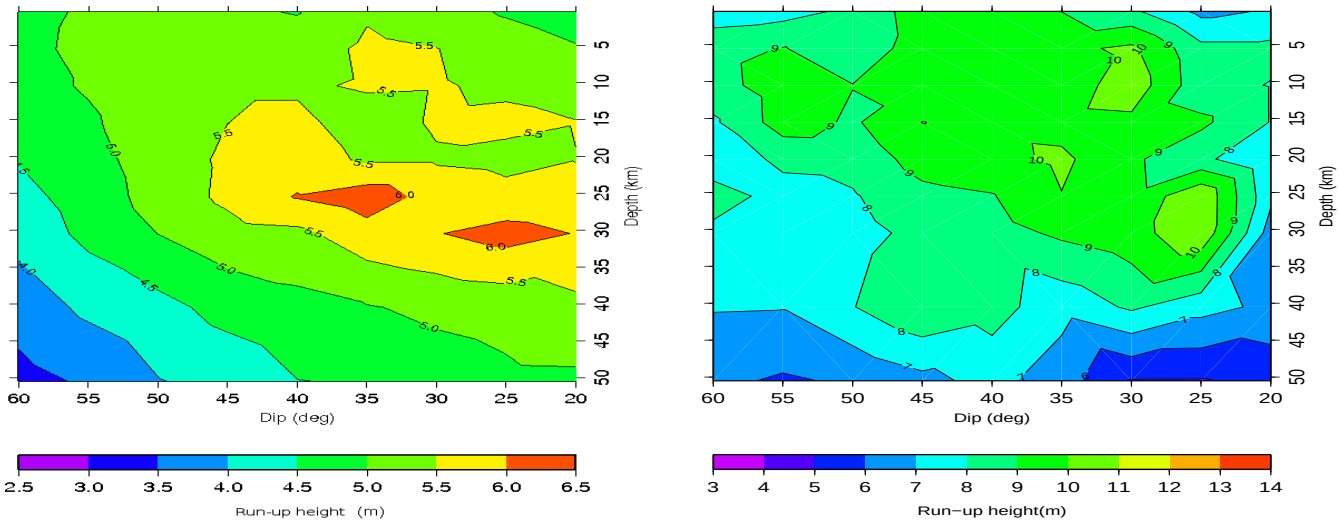

(a) (b)

Figure 4.15: *Run-up at the Central/Ria zone. (a) AnuGA e (b) COMCOT. (see figure 4.6 for zone bounds).*

In the Central/Ria zone (figure 4.15) AnuGA has the same behaviour as in the West/Lagos zone but with a 0.5 to 1 m higher *run-up* than the latter. In the COMCOT model, maximum values are now located on the lower and intermediate depths (between 5 and 30 km) and on the sources with an intermediate dip angle (between 25 and 40°).

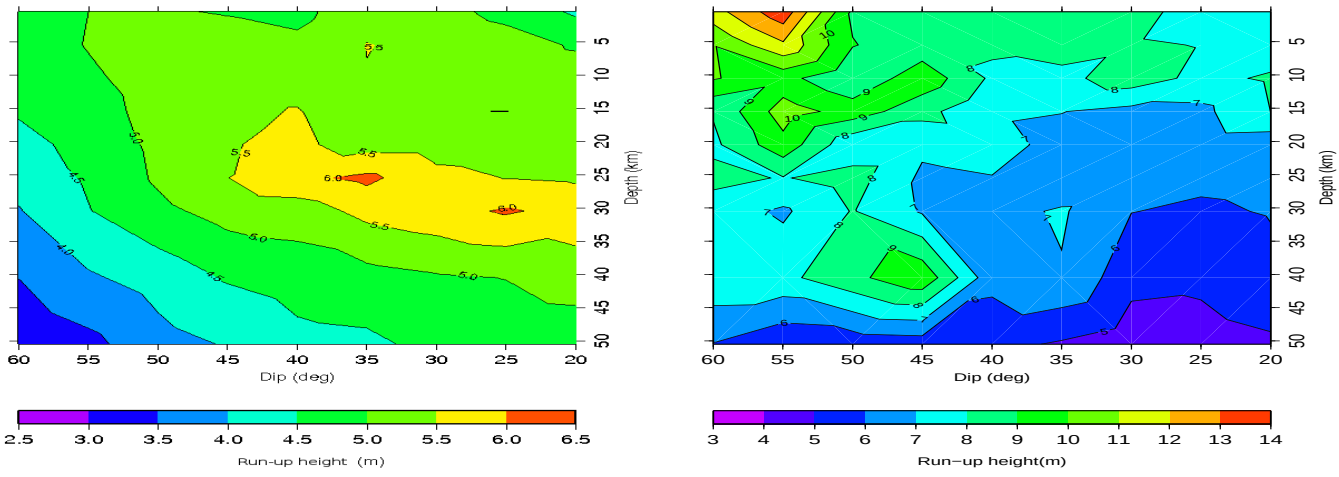

(a) (b)

Figure 4.16: *Run-up at the East/Alvor zone. (a) AnuGA e (b) COMCOT. (see figure 4.6 for zone bounds).*

Figure 4.16 shows the results obtained in the East/Alvor zone. Model AnuGA displays results with the same magnitude as the ones at the Central/Ria zone. COMCOT produces for this zone the highest *run-up* of all runs between 13 and 14 m. In this zone maxima are attained in the shallower depths (between 5 and 25 km) and higher dip angles (between 45 and 60°). For higher dip angles there is less variation of the *run-up* than for the lower dip angles.

Table 4.4 summarizes the highest *run-up* results obtained in each analysis zone.

	AnuGA			COMCOT		
zone	dip angle (^{o})	fault depth (km)	*run-up* (m)	dip angle (^{o})	fault depth (km)	*run-up* (m)
West/Lagos	35	25.5	5.88	55	10.5	9.5
Central/Ria	35	25.5	6.27	25	25.5	10.83
East/Alvor	35	25.5	6.11	55	0.5	13.69

Table 4.4: *Highest run-up in each analysis zone of Alvor.*

For each model we have chosen from table 4.4 the case of highest *run-up*. Next we will present the inundation maps obtained using both cases and also the wave heights at gauge #15. For AnuGA we chose the case with a fault model of a dip angle of 35° and depth of 25.5 km. For COMCOT we chose the case with a fault model of a dip angle of 55° and depth of 0.5 km that corresponds to the highest *run-up* modelled.

The next two figures show the inundation maps just referred to. The first is figure 4.17a and corresponds to the maps obtained with a fault model of a dip angle of 35° and depth of 25.5 km. On top we can observe the wave at gauge #15 just before inundation. The first inundation map was obtained with AnuGA and the second map from COMCOT for the same fault model. The second figure (4.18a) corresponds to the maps obtained with a fault model of a dip angle of 55° and depth of 0.5 km. On top is the wave gauge #15. The first map was obtained with COMCOT and the second with AnuGA for the same fault model.

Run-in

The *run-in* results will be analysed on four areas. The West/Lagos zone was divided in two distinct areas. The first is mentioned forward as marina area and encloses the Lagos marina inlet. The second area is mentioned forward as Meia-praia area and encloses the beach environment with a dune field in the West/Lagos zone. The Central/Ria zone was maintained as is. The East/Alvor zone was modified in order to exclude the small part of the "Ria" branch at the western tip of the zone. The areas described are identified in red on figure 4.6.

The figure 4.19 shows the *run-in* results. AnuGA tends to concentrate the results on the 600 to 700 m strip for almost all the source parameters tested. COMCOT produces maximum *run-in* values between 900 and 1000 m, occurring with source parameters of intermediate dip angle (between

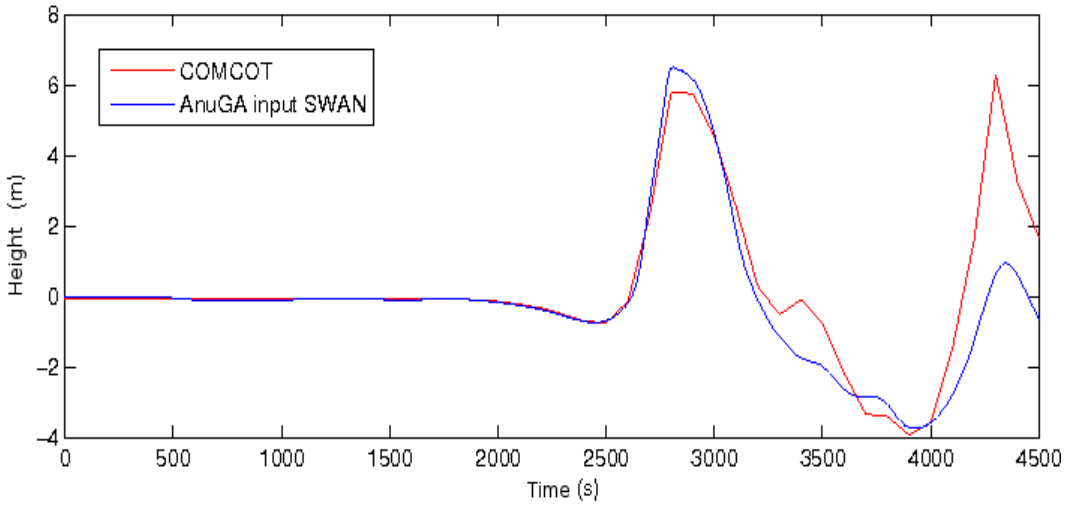

(a)

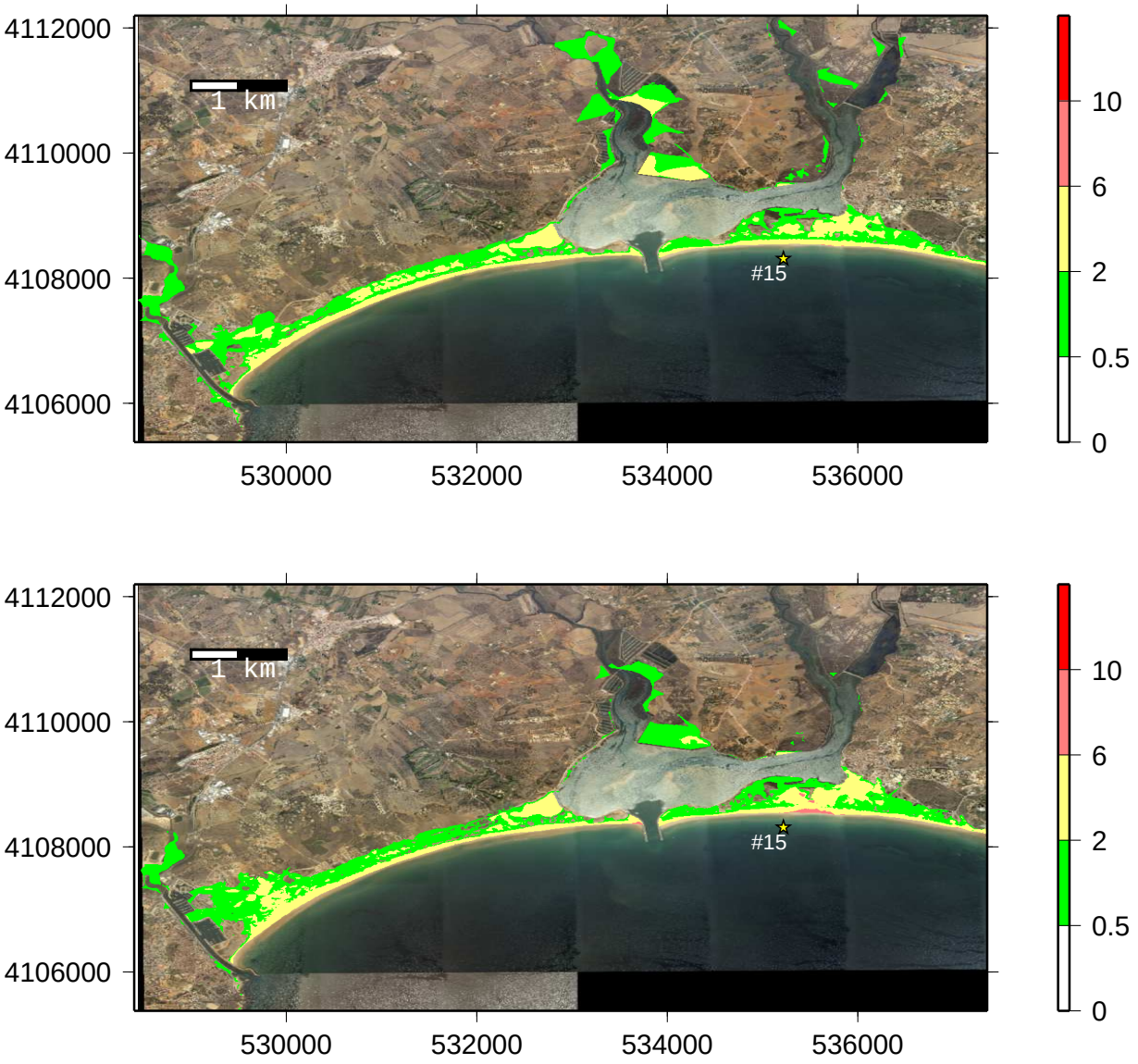

(b)

Figure 4.17: *(a) Water heights at gauge #15 for both models. (b) Two inundation maps for the highest run-up modelled with AnuGA, fault model with a dip angle 35º and fault depth of 25.5 km. First map is in meters and was obtained with AnuGA. The second map is in meters and was obtained with COMCOT for the same source model.*

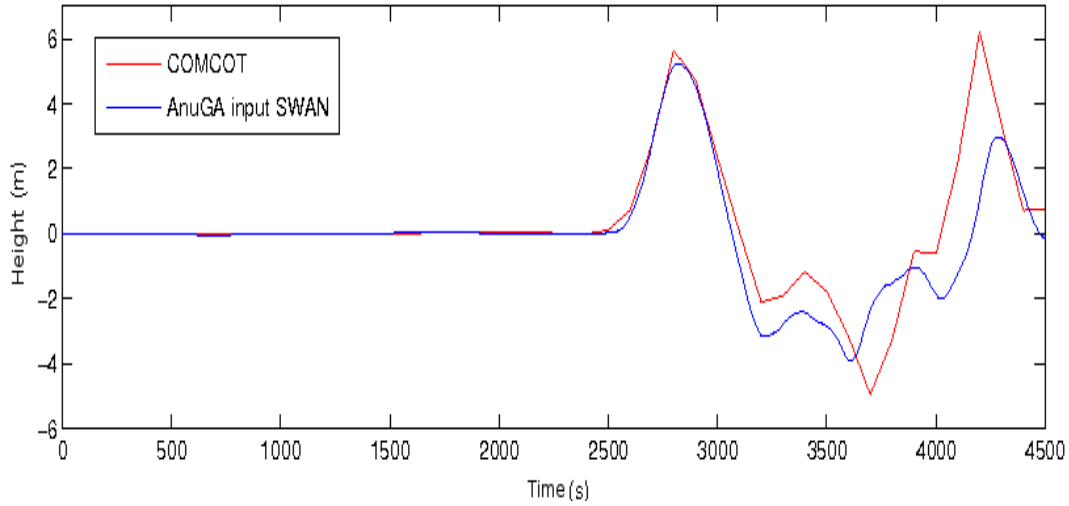

(a)

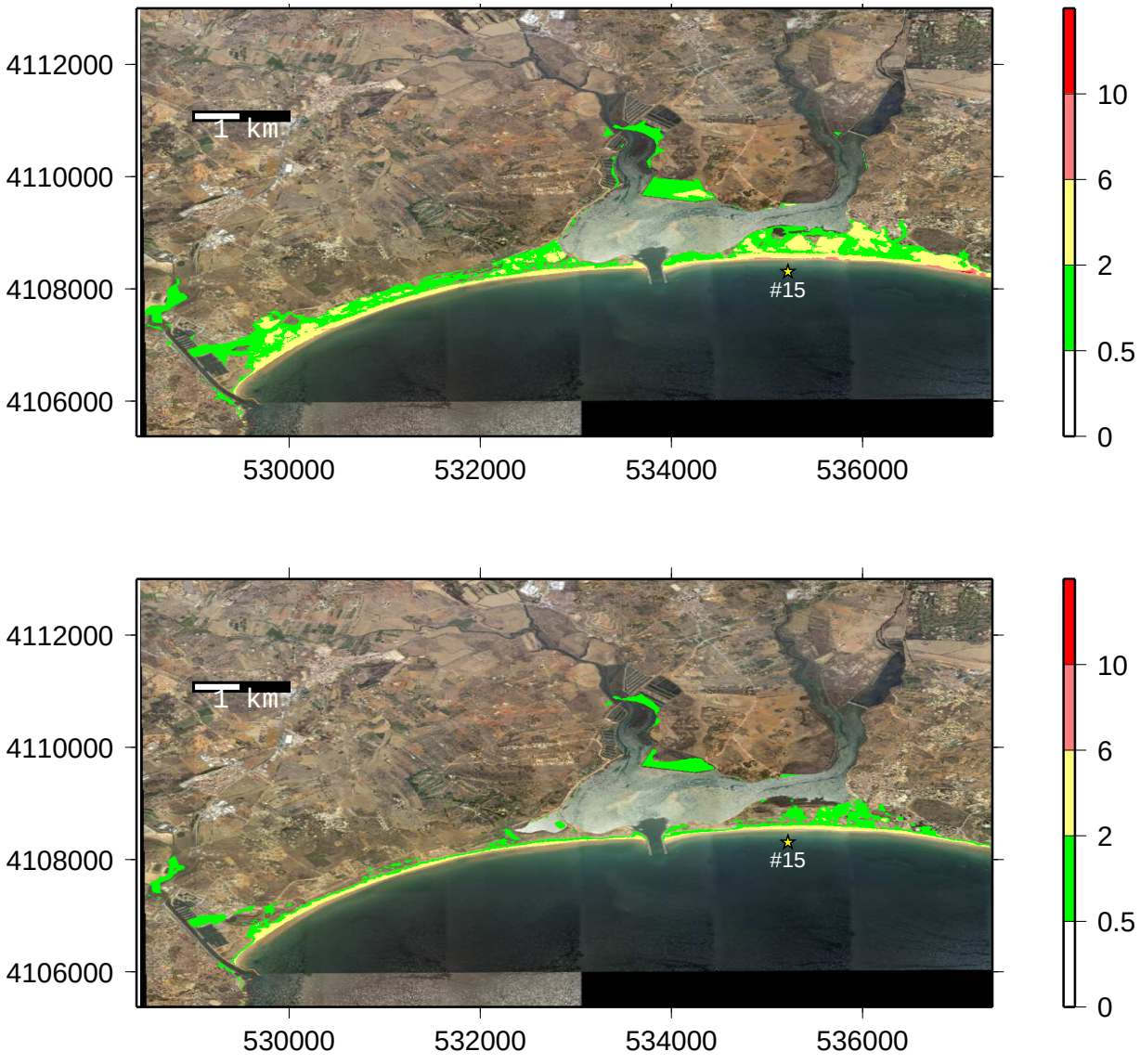

(b)

Figure 4.18: *(a) Water heights at gauge #15 for both models. (b) Two inundation maps for the highest run-up modelled with COMCOT, fault model with a dip angle 55^o and fault depth of 0.5 km. First map is in meters and was obtained with COMCOT. The second map is in meters and was obtained with AnuGA for the same source model.*

30 and 40°) and depths between 5 and 35 km. Outside this region the *run-in* decreases to values of approximately 600 m.

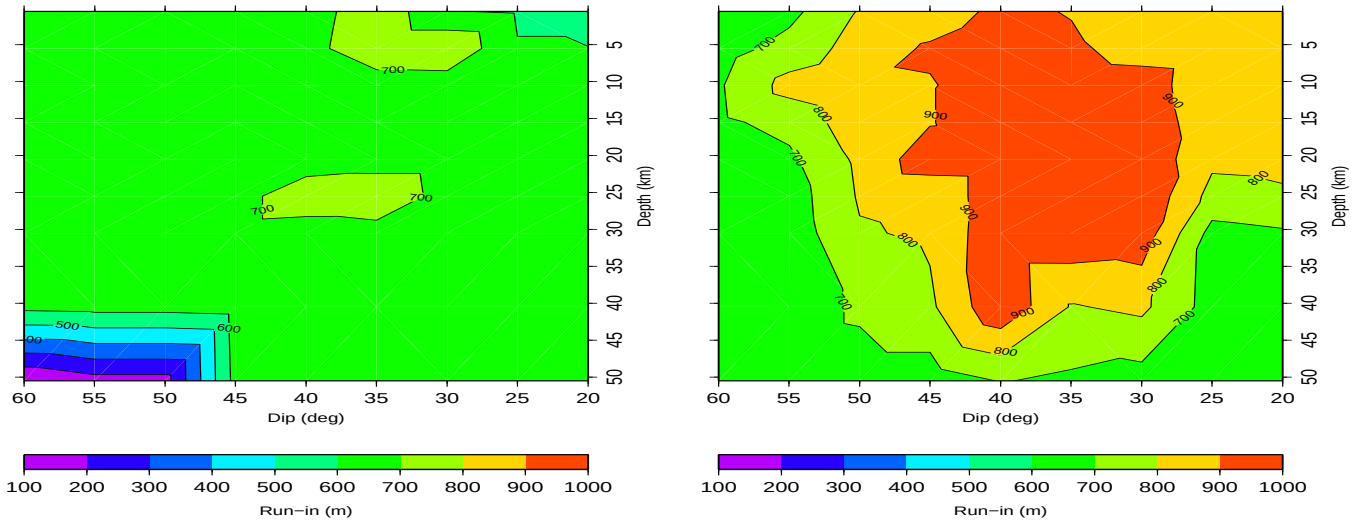

(a) (b)

Figure 4.19: *Run-in results for the West/Lagos zone, Meia-Praia area. (a) AnuGA. (b) COMCOT.*

The figure 4.20 shows the *run-in* results obtained at the marina area in the West/Lagos zone. The models are mutually consistent, concentrating their results on few intervals. COMCOT predicts a maximum between 2250 and 2500 m occurring with dip angles between 20 and 30° and depths between 5 and 15 km. The remaining cases fall in the range of 1500 to 2000 m. AnuGA predicts an extreme *run-in* case more than 2250 m with a dip angle of 35° and depth of 25.5 km. The remaining cases fall on the strip between 1500 and 2000 m. The existence of the marina inlet and tidal channels allows water to enter easily and penetrate long distances.

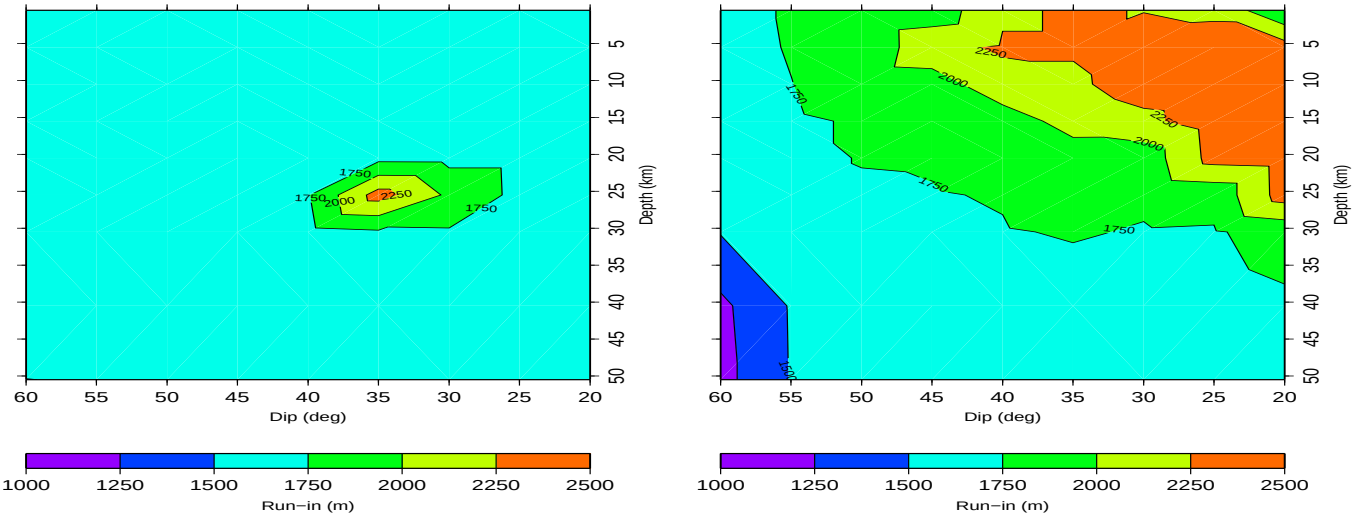

(a) (b)

Figure 4.20: *Run-in results for the West/Lagos zone, Marina area. (a) AnuGA. (b) COMCOT.*

The figure 4.21 shows the results in the Central/Ria zone. These results have the same charac-

teristics as the ones in the marina area since this environment has also an inlet that allows water to enter uninpeded. The COMCOT *run-in* results can be grouped in two ranges. The first (between 2500 and 2750 m) occurs for source parameters of high dip angle at almost all depths. The second group (between 4000 and 4250 m) occurs for source parameters of low dip angle and shallower fault depths. Most of the results obtained with AnuGA are grouped in range from 3250 and 3500 m. It predicts a higher *run-in* with source parameters of a low and intermediate angle and fault depths between 15 and 40 km. The maximum obtained in this group is 4546 m obtained with a dip angle of 30° and 15.5 km.

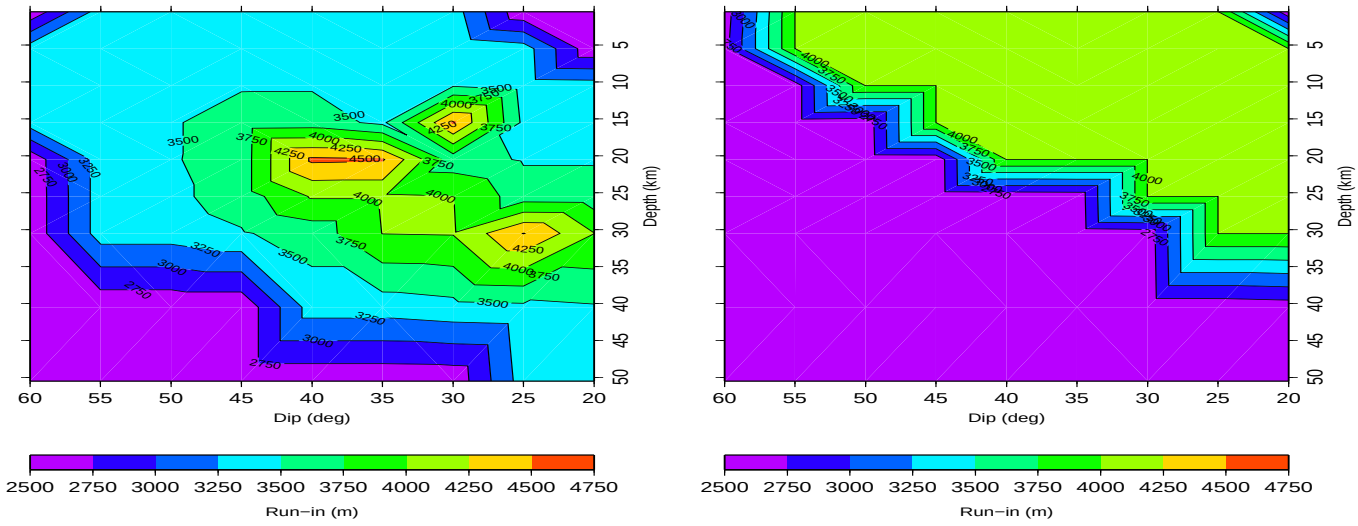

(a) (b)

Figure 4.21: *Run-in results for the Central/Ria zone. (a) AnuGA. (b) COMCOT.*

Figure 4.22 shows the results obtained in the East/Alvor zone. COMCOT's *run-in* results are affected by the source model's fault depth. For shallower and intermediate depths (between the 5 and the 25 km) the *run-in* is in the range of 750 to 850 m, except for a maximum that occurs with a dip angle of 45^o and a depth of 5 km and has a value of 950 m. For deeper fault depths (more than 25 km) the *run-in* ranges from 650 to 750 m. In model AnuGA the *run-in* results are more dependent on the dip angle than on fault depth. The lowest *run-in* values occur with source parameters of high dip angle and deep fault depths. The *run-in* in these cases is below 450 m. Cases with a low dip angle have the highest *run-in* with values between 550 and 750 m.

Table 4.5 summarizes the maximum *run-in* values obtained at each of the analysis zones. From the table we have chosen a case for each numerical model to plot the maximum inundation extents on a map of the study area. The criterion was the highest *run-in* value obtained with each of the two numerical models. The Central/Ria zone was excluded since it is an area with a direct connection to the sea. For AnuGA it was chosen the run with the source parameters dip of 35° and depth of 25.5 km. For COMCOT we chose the run with the source parameters dip angle of 20° and fault depth of 15.5 km. Figures 4.24 and 4.25 compare the inundation extents derived from AnuGA's

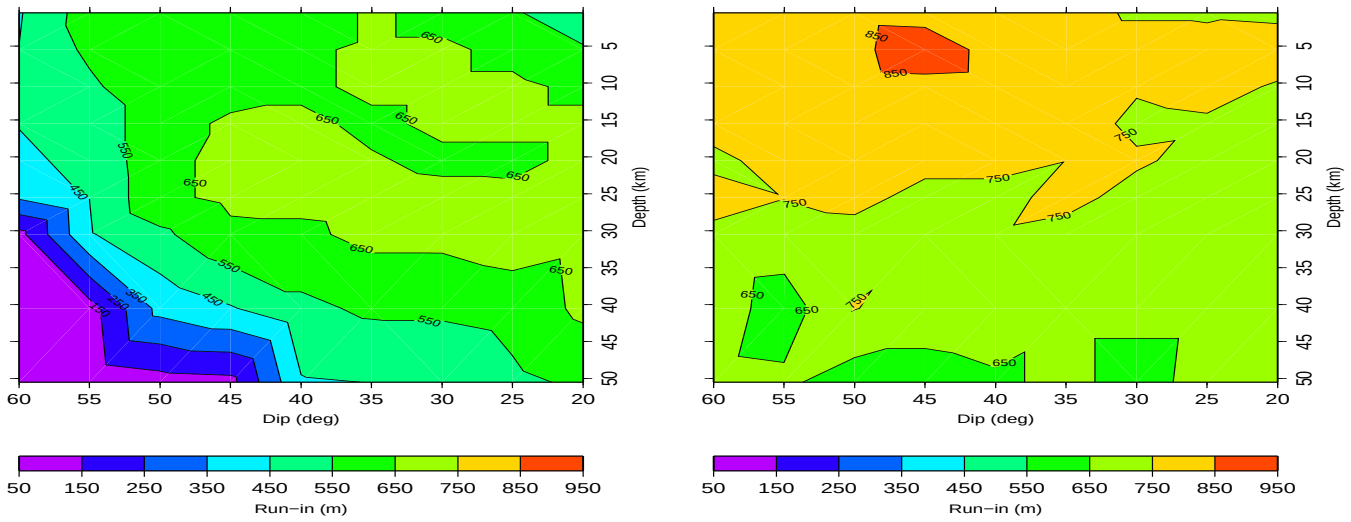

(a) (b)

Figure 4.22: *Run-in results for the East/Alvor zone. (a) AnuGA. (b) COMCOT.*

	AnuGA			COMCOT		
zone	dip angle (^{o})	fault depth (km)	*run-in* (m)	dip angle (^{o})	fault depth (km)	*run-in* (m)
West/Lagos - Marina	35	25.5	2356	20	15.5	2378
West/Lagos - Meia-praia	30	5.5	792	30	25.5	988.4
Central/Ria	30	15.5	4546	20	5.5	4004.3
East/Alvor	25	30.5	709.36	45	5.5	950

Table 4.5: *Highest run-in for each analysis zone at Alvor.*

and COMCOT's results based on these parameters.

Amplification factor

The amplification factor is the ratio between the maximum water height near the shoreline and the maximum water height at the source. The first is measured at gauges placed on the 5 m isobath and the second directly above the source using a perpendicular profile.

Figure 4.23 shows the amplification factor results. The amplification factor depends more on the fault's depth than the fault's dip angle. Both COMCOT and AnuGA input with SWAN configurations present smaller factors at shallower depths. The threshold from a decreasing factor to a gain on wave height occurs at 20 km depth for AnuGA and at 5 km depth for COMCOT. With depth increase COMCOT presents a higher amplification factor for steeper dip angles while AnuGA presents a higher factor for lower angles.

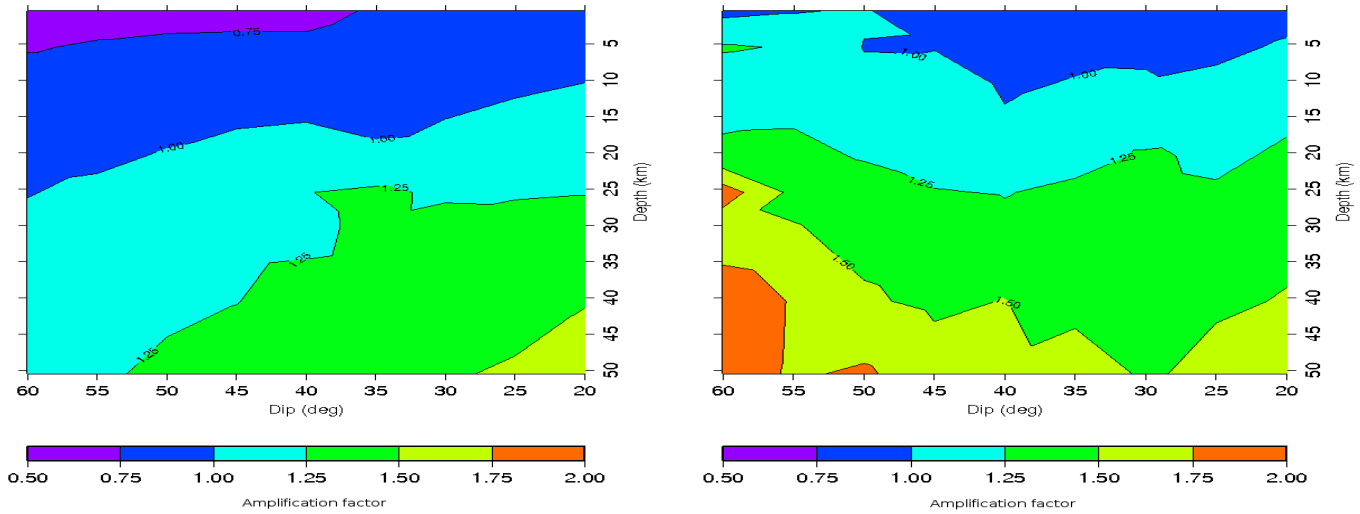

(a) (b)

Figure 4.23: *Amplification factors between the maximum water height at the 5 m isobath and the maximum water height at the source. (a) AnuGA. (b) COMCOT.*

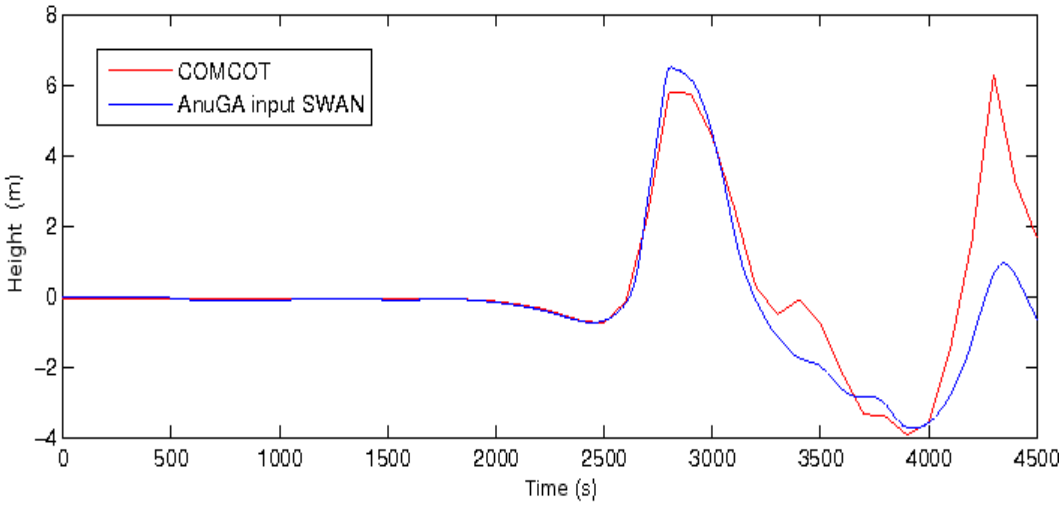

(a)

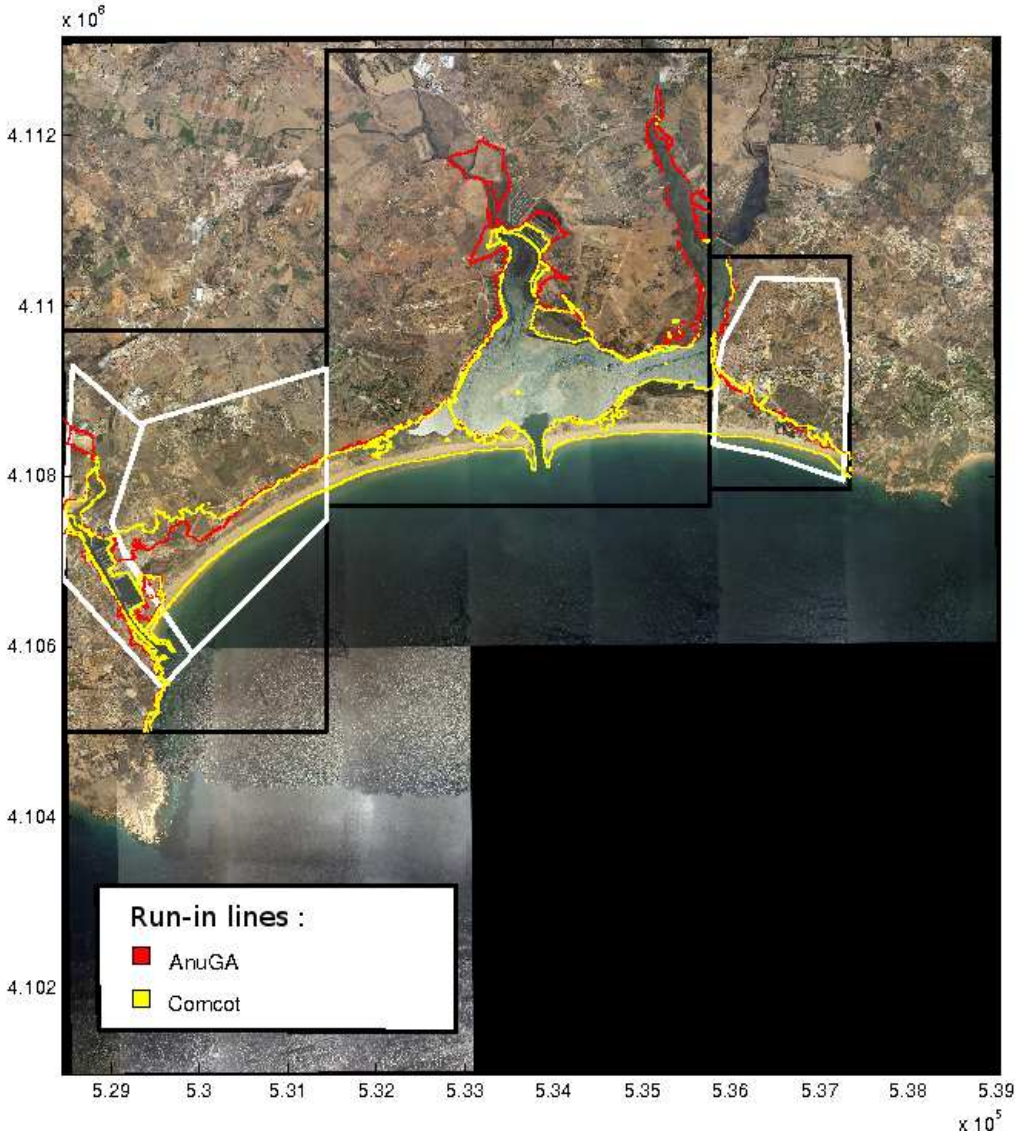

(b)

Figure 4.24: *(a) Water height at gauge #15 for both models. (b) Inundation extents plotted on aerial photograph of the study area. Inundation with source model dip 35º and depth 25.5 km. Red inundation line - obtained with AnuGA; Yellow inundation line - obtained with COMCOT; Maximum values at the West/Lagos - Marina zone. (Aerial photography from IPCC/DGRF 2005).*

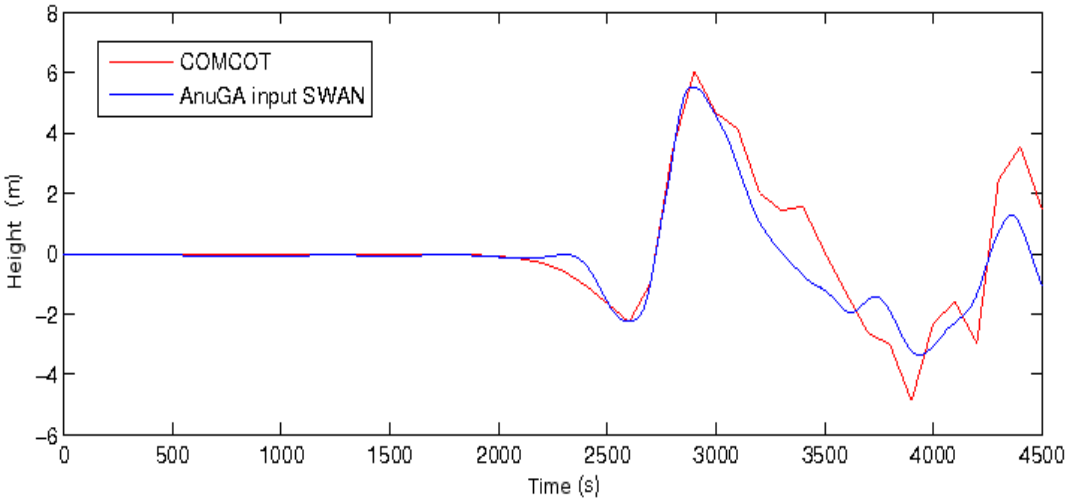

(a)

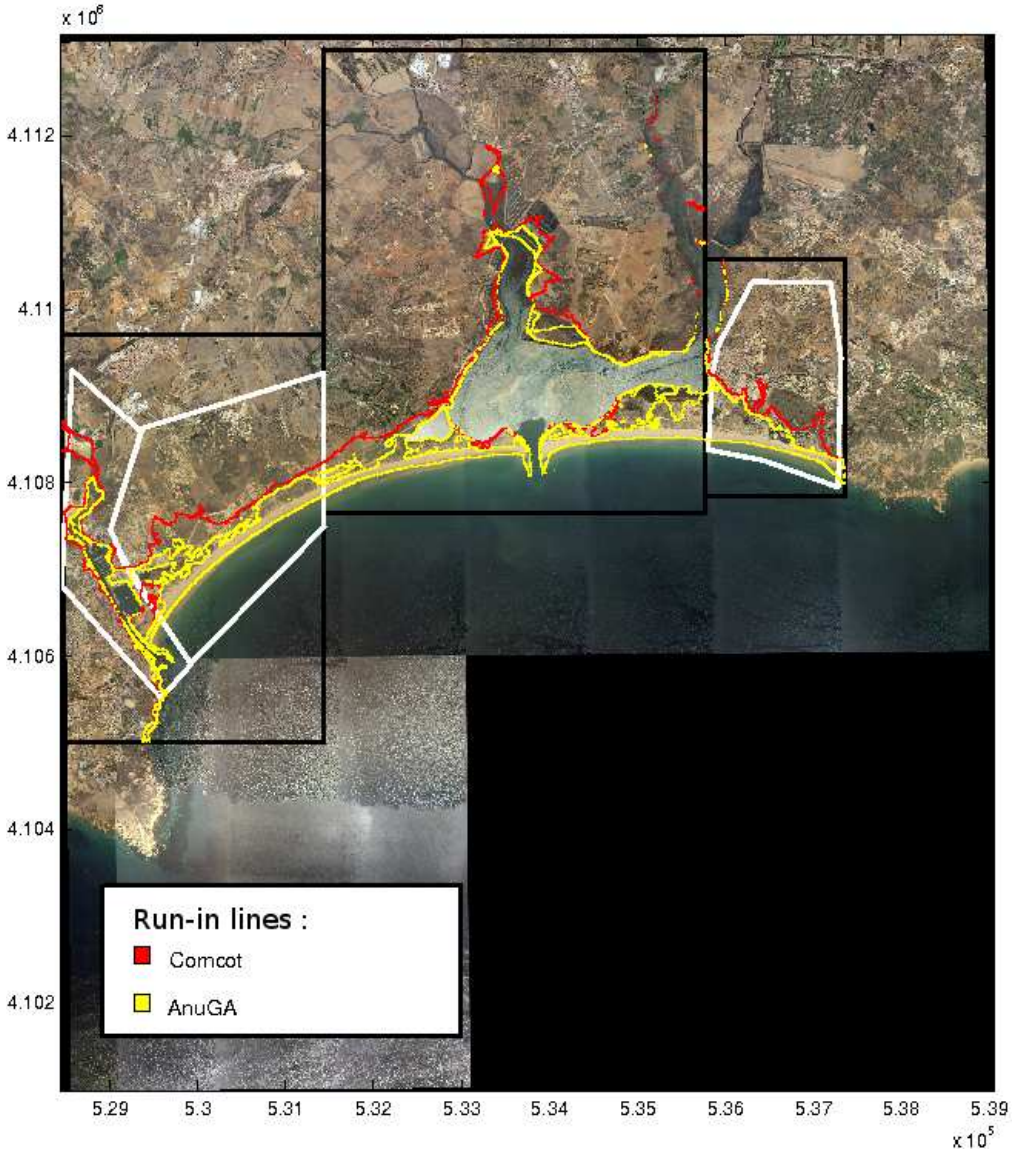

(b)

Figure 4.25: *(a) Water height at gauge #15 for both models. (b) Inundation extents plotted on aerial photograph of the study area. Inundation with source model dip 20º and depth 15.5 km. Red inundation line - obtained with COMCOT; Yellow inundation line - obtained with AnuGA; Maximum values at the West/Lagos - Marina zone. (Aerial photography from IPCC/DGRF 2005).*

Chapter 5

Analysis

5.1 Boca do Rio

5.1.1 Model adjustment to the Algarve coast

The purpose of using the Boca do Rio test case was to model a similar event to the 1755 one, in order to understand if the results achieved were in agreement with the historical data collected. We have found a good agreement between the modelled and the historical data leading to the conclusion that the grid coupling method of COMCOT and the finite volume method of AnuGA are adapted to the Algarve's coast.

5.1.2 Model configurations

Of the configurations tested in AnuGA, inputting with model SWAN has demonstrated to be an adequate solution. The differences of the wave forms at the boundaries (figures 3.6 and 3.7) and the wave form at the 5 m isobath (figure 3.9b) are not significant. The differences in maximums are of 0.45 and 0.5 m at the west and south boundaries and the linear correlation is of 0.96 and 0.97, respectively. This difference augments to 1 m at the 5 m isobath, where the correlation is of 0.87. Nevertheless, the differences continue not to be substantial and do not seem to influence the inundation since the results achieved are very similar between both cases (see table 3.3).

The analysis of COMCOT configurations has to be divided in two parts: the propagation and the inundation. On the first, using linear or non-linear equations has not revealed important differences near the shoreline (see figure 3.9c). Here the non-linear equations wave is 1 m higher than the linear equations one and the linear correlation is of 0.79.

On the second, regarding inundation, COMCOT with linear equation registers a distinct behaviour, producing *run-up* and *run-in* results 50% higher than other configurations. Moreover, the water level on land increases with linear equations and diminishes with non-linear equations, as can be observed on the cross-shore profile in figure 3.8. This behaviour was not expected and as it was not possible to find documentation regarding this option, it was not possible to understand the reason for this behaviour.

5.2 Alvor

The *run-up* and *run-in* results for the Alvor test area produced by COMCOT are always higher than those calculated by AnuGA. This difference seems to be in the inundation since a good agreement is found in the propagation from the source to the 5 m isobath between COMCOT and AnuGA. The gauges on figures 4.17a, 4.18a, 4.24a and 4.25a compare COMCOT and AnuGA inputted with SWAN at the 5 m isobath where linear correlations of 0.86 to 0.90 were obtained.

The results obtained with the finite volume inundation method of AnuGA have been more consistent than those with the moving boundary method of COMCOT. For the analysis zones used, the maximum *run-up* and *run-in* results of AnuGA has been observed with source models very proximate while for COMCOT different source models have obtained maximum *run-up* results at each zone.

The source model parameters have revealed a differentiated influence on each code. Anuga's highest inundations have occurred for source models with a depth around 30 km while in COMCOT were the shallowest source models that have revealed the most capacity to flood but the results are more disperse in this case (see tables 4.4 and 4.5). Important differences have been found when comparing the maximum *run-up* and *run-in* of COMCOT versus its corresponding in AnuGA for the same source model parameters (figures 4.18 and 4.25). This point raises the question of which model better reproduces reality.

Chapter 6

Conclusion

The main goals of the Boca do Rio test case were fulfilled and allowed a better comprehension of both model's options which were the basis of the choices made for the Alvor test case. Also, the good adaption of the models to the Algarve's coast was obtained with this test case.

Inputting AnuGA with the variation of the free surface elevation and momentum from models COMCOT and SWAN hasn't shown significant differences. Therefore, we have chosen to use AnuGA inputted with SWAN which can be obtained with significant less computational effort and time consumption. Average CPU time for a COMCOT complete model run was of 10 hours with inundation included on a Intel Core 2 Quad CPU with 2.66 Ghz and 2 Gb of RAM while a complete SWAN without inundation run took approximately 40 min. Even though a direct comparison of times was not possible, the difference is considerable.

Taking advantage of the a multibeam survey available at Alvor, a comparison of using this dataset for the composing the bathymetric elevation data versus using the dataset contracted for project ERSTA, a bathymetric survey from IH, was performed. The results have shown little differences on the wave forms from using each of the datasets. The zone were the comparison was performed is not composed of a rugged morphology as figure 4.11 indicates.

Regarding the results achieved with the Alvor test case have shown a good agreement between the propagation of model COMCOT and model AnuGA inputted with SWAN. The differences found in the *run-up* and *run-in* results seem to be derived from the inundation methods used by the models, the finite volume by AnuGA and the moving boundary by COMCOT.

Future Work

When analyzing the results of Alvor, the question of which numerical model better represents reality was raised. It was not possible to answer this question with the synthetic cases used in Alvor test case neither with the Boca do Rio test case. Even though the latter is supported on real data, care must be taken on its analysis since: there isn't gauge data from the real event available for comparison; the historical reports collected are based on observations and are not 100% trustworthy; and the topographic and bathymetric data used to model this event does not necessarily match the topography of the historical data.

References

[1] *COMCOT: Background Theory.* Webpage accessed: August 2008. URL `http://ceeserver.cee.cornell.edu/pll-group/comcot_bg.htm`.

[2] *Integrated observations from NEAR shore sourcES of Tsunamis: towards and early warning system (NEAREST).* Website accessed: January 2009. URL `http://nearest.bo.ismar.cnr.it`.

[3] *SEismic and tsunami risk Assessment and mitigation scenarios in the western HELLenic ARC (SEAHELLARC).* Website accessed: January 2009. URL `http://seahellarc.gr`.

[4] *Seismic eArly warning For EuRope (SAFER) project.* Website accessed: January 2009. URL `http://www.saferproject.net/index.htm`.

[5] *Tsunami Risk ANd Stratagies For the European Region (TRANSFER).* Website accessed: January 2009. URL `http://www.transferproject.eu`.

[6] ANPC (2005). *Seminar on Early Warning Systems.* Webpage accessed: January 2009. URL `http://www.proteccaocivil.pt/ews`.

[7] Baptista, M. A. *et al.* (1998). *The 1755 Lisbon Tsunami; Evaluation of the tsunami parameters.* Journal of Geodynamics, 25, pp. 143–157.

[8] Baptista, M. A. *et al.* (1998). *Constraints on the source of the 1755 Lisbon tsunami inferred from numerical modelling of historical data on the source of the 1755 Lisbon tsunami.* Journal of Geodynamics, 25, pp. 159–174.

[9] Baptista, M. A. *et al.* (2003). *New study of the 1755 earthquake source based on multi-channel seismic survey data and tsunami modeling.* Natural Hazards and Earth System Sciences, 3, pp. 333–340.

[10] Baptista, M. A. *et al.* (2006). *Tsunami Propagation Along Tagus Estuary (Lisbon, Portugal) Preliminary Results.* Science of Tsunami Hazards, 24 - NÂº 5, pp. 329–338.

[11] Bernard, E. N. *et al.* (2006). *Tsunami: scientific frontiers, mitigation, forecasting and policy implications.* Phil. Trans. R. Soc. A, 364, pp. 1989–2007.

[12] Billing, P. (2007). *State of the Art on Early Warning Systems.* Communication to Seminar on Early Warning Systems, Albufeira, Portugal.

[13] Comission, E. *Indian Ocean Tsunami - The EU Response.* Website accessed: January 2009. URL `http://ec.europa.eu/world/tsunami/disaster_response/memo05_136.htm`.

[14] Courant, R. *et al.* (1967). *On the partial difference equations of mathematical physics.* IBM Journal, pp. 215–234. English translation of the 1928 German original.

[15] George, D. L. (2006). Finite Volume Methods and Adaptive Refinement for Tsunami Propagation and Inundation. Ph.D. thesis, University of Washington.

[16] Hindson, R. and Andrade, C. (1999). *Sedimentation and hydrodynamic processes associated with the tsunami generated by the 1755 Lisbon earthquake.* Quaternary International, 56, pp. 27–38.

[17] Hindson, R. A. *et al.* (1996). *Sedimentary Processes Associated with the Tsunami Generated by the 1755 Lisbon Earthquake on the Algarve Coast, Portugal.* Physical Chemical Earth, 21, pp. 57–63.

[18] Inamura, F. (1997). Tsunami Numerical Simulation with the Staggered Leap-Frog Scheme (Numerical Code of TUNAMI-N1 and N2). Disaster Control Research Center, 33 pp.

[19] Kerridge, D. (2005). *The threat posed by tsunami to the UK.* Tech. rep., Study commissioned by Defra Flood Management and produced by British Geological Survey, Proudman Oceanographic Laboratory, Met Office and HR Wallingford.

[20] LeVeque, R. J. (1997). *Wave Propagation Algorithms for Multidimensional Hyperbolic Systems.* Journal of Computational Physics, 131, pp. 327–335.

[21] Liu, P. F. *et al.* (1994). Numerical Simulations of the 1960 Chilean Tsunami Propagation and Inundation at Hilo Hawaii In: El-Sabh, M.I. (ed.), Recent Development in Tsunami Research. Kluwer Academic Publishers.

[22] Liu, P. L.-F. *et al.* (1998). Computer Programs for Tsunami Propagation and Inundation - Technical Manual. School of Civil and Environmental Engineering, Cornell University Department of Civil Engineenring and Institute of Waterway Industry, Sejong University, Seul.

[23] Lopes, J. S. (1841). Corografia ou Memória Económica , Estadística e Topográfica do Reino do Algarve. Typográfica Real da Academia das Sciencias.

[24] Luis, J. F. (2007). *Mirone: A multi-purpose tool for exploring grid data.* Computers & Geosciences, 33, pp. 31–41.

[25] Mader, C. L. (2004). Numerical Modeling of Water Waves. CRC Press, 2nd edn., 288 pp.

[26] Mansinha, L. and Smylie, D. E. (1971). *The displacement fields of inclined faults.* Bulletin of the Seismological Society of America, 61, pp. 1433–1440.

[27] Matsuyama, M. and Tanaka, H. (2001). *An experimental study of the highest run-up height in the 1993 Hokkaido Nansei-Oki earthquake tsunami.* In ITS 2001 Proceedings.

[28] Nations, U. *Resolution on the Hyogo Framework for Action 2005-2015: Building the Resilience of Nations and Communities to Disasters.* adopted on 22 January 2005 by the World Conference on Disaster Reduction (A.CONF.206/6).

[29] Nielsen, O. (2007). ANUGA v1.0 User Manual. Geoscience Australia and the Australian National University.

[30] Nielsen, O. *et al.* (2005). *Hydrodynamic modelling of coastal inundation.* In Proc. Int. Congress on Modelling and Simulation, pp. 518–523.

[31] Oliveira, C. S. (2007). *Study on the risk of earthquakes and tsunamis in the Algarve Region (Portugal).* Communication to Seminar on Early Warning Systems, Albufeira, Portugal.

[32] Papadopoulos, G. A. (1998). *A tsunami catalogue of the area of Greece and adjacent seas.* Tech. Rep. Publication Number 8, Institute of Geodynamics, National Observatory of Athens. 17 pp.

[33] Richardson, K. (2006). *Tsunamis - assessing the hazard for the UK and Irish coast.* Tech. rep., Department for Environment Food and Rural Affairs.

[34] Sexton, J. (2006). *Geoscience Australia's impact modelling protecting Australia.* Article in AusGEO News, 83.

[35] Shewchuk, J. *Triangle - A Two-Dimensional Quality Mesh Generator and Delaunay Triangulator.* Webpage accessed: August 2008. URL `http://www.cs.cmu.edu/~{}quake/triangle.html`.

[36] Silva, P. (2004). *Modelacão numérica da propagacão de ondas Tsunami e sua interaccão com a região costeira de Faro.* Relatório do projecto técnico científico da Licenciatura em Oceanografia da Universidade do Algarve (in portuguese).

[37] de Sousa, P. (1919). O Terramoto de 1Âº de Novembro de 1755 em Portugal, um estudo demogrÃ¡fico, vol. I e II. ServiÃ§os Geológicos de Portugal.

[38] Synolakis, C. *et al.* (2007). *Standards, criteria, and procedures for NOAA evaluation of tsunami numerical models.* NOAA Tech. Memo OAR PMEL-135, NOAA/Pacific Marine Environmental Laboratory, Seattle, WA.

[39] Tinti, S. (1993). *The project GITEC: a European effort to address tsunami risk.* In P. A. Meriman, C. W. A. Browitt and R. Society, eds., Natura Disasters: Protecting Vulnerable Communities: Proceedings of the Conference Held in London. Thomas Telford.

[40] Tinti, S. *et al.* (1998). *The unified European catalog of tsunamis: A GITEC experience.* In International Conference on Tsunamis, Paris, pp. 83–99.

[41] Titov, V. V. and Gonzalez, F. (1997). *Implementation and testing of the Method of Splitting Tsunami (MOST) model.* Tech. rep., NOAA Technical Memorandum ERL PMEL-112.

[42] University, C. (2004). *The Third International Workshop on Long-Wave Runup Models.* Webpage accessed: February 2008. URL `http://www.cee.cornell.edu/longwave/`.

[43] Wang, X. and Liu, P. L. (2006). *An analysis of 2004 Sumatra earthquake fault plane mechanisms and Indian Ocean tsunami.* Journal of Hydraulic Research, 44, pp. 147–154.

[44] Weisstein, E. W. *"Euler Forward Method" from MathWorld – A Wolfram Web Resource.* Website accessed: January 2009. URL `http://mathworld.wolfram.com/EulerForwardMethod.html`.

[45] Wessel, P. and Smith, W. H. F. (1991). *Free software helps map and display data.* In EOS Transactions AGU, vol. 72, pp. 441–441.

Appendix A: AnuGA script run_alvor.py

```
"""Script for running a tsunami inundation scenario for Alvor.
"""
#-----------------------------------------------------------------------
# Import necessary modules
#-----------------------------------------------------------------------

# Standard modules
import os
import time
import sys

# Related major packages
from anuga.shallow_water import Domain
from anuga.shallow_water import Transmissive_boundary
from anuga.shallow_water import Reflective_boundary
from anuga.shallow_water import Dirichlet_boundary
from anuga.shallow_water import Time_boundary
from anuga.shallow_water import File_boundary
from anuga.shallow_water import Field_boundary

from anuga.pmesh.mesh_interface import create_mesh_from_regions
from anuga.shallow_water.data_manager import convert_dem_from_ascii2netcdf
from anuga.shallow_water.data_manager import dem2pts
from anuga.shallow_water import Transmissive_Momentum_Set_Stage_boundary
from anuga.abstract_2d_finite_volumes.util import file_function

from anuga.caching import cache
from anuga.utilities.polygon import read_polygon, plot_polygons, \
                                    polygon_area, is_inside_polygon
```

```
def run_alvor(fault_filename,out_filename,tide_,simulation_time, \
                                        resolucao_temporal,friction_):
    #------------------
    # Initial condition
    #------------------
    tide = tide_
    friction = friction_

    dem_name = 'alvor_10m'
    meshname = 'alvor.msh'
    basename = 'alvor'

    path_fault = '../../swan/'
    path_data = '../dados/'
    data_filename = 'alvor_10m.pts'

    print 'Files:'
    print 'Fault: '+ path_fault + fault_filename
    print 'Data: ' + path_data + data_filename
    print 'Output filename: ' + out_filename

    # bounding polygon for study area
    bounding_polygon = read_polygon(path_data + 'out_alvor.csv')
    # interior polygons
    poly_shallow = read_polygon(path_data + 'poly_shallow.csv')
    poly_bat = read_polygon(path_data + 'poly_bat.csv')
    poly_interior = read_polygon(path_data + 'poly_interior.csv')

    #------------
    # Resolutions
    #------------
    remainder_res = 10000
    bat_res = 2500
    interior_res = 500
    shallow_res = 100
    interior_regions = [[poly_bat, bat_res],[poly_shallow, shallow_res],\
                                        [poly_interior, interior_res]]

    # ---------------------
    # Function to be cached
    # ---------------------
```

```
def setup_domain(tide, bounding_polygon, remainder_res,\
                            interior_regions, mesh_filename, \
                                    points_filename, friction):

    # Mesh with 4 boundaries
    create_mesh_from_regions(bounding_polygon,
                         boundary_tags={'west': [0],
                                        'north': [1],
                                        'east': [2],
                                        'south': [3]},
                         maximum_triangle_area=remainder_res,
                         filename=mesh_filename,
                         interior_regions=interior_regions,
                         use_cache=False,
                  verbose=True)

    #--------------------------------------------------------------
    # Setup computational domain
    #--------------------------------------------------------------

    domain = Domain(mesh_filename,
                    use_cache=False,
                    verbose=True)

    print 'Number of triangles = ', len(domain)
    print 'The extent is ', domain.get_extent()
    print domain.statistics()

    domain.set_name(basename)
    domain.set_quantities_to_be_stored(['stage', 'xmomentum',\
                                                    'ymomentum'])
    domain.set_minimum_storable_height(0.01)

    #--------------------------------------------------------------
    # Setup initial conditions
    #--------------------------------------------------------------
    domain.set_quantity('stage', tide)
    domain.set_quantity('friction', friction)
    domain.set_quantity('elevation',
                        filename=points_filename,
```

```
                        use_cache=False,
                        verbose=True)
    return domain

# ------------------------ End Function to be cached -------------

#--------------------------------
# Call (and cache) setup function
#--------------------------------
# Run set_up domain with caching
domain = cache(setup_domain,(tide,bounding_polygon,remainder_res,\
                                        interior_regions,meshname,
                                path_data+data_filename, friction),\
                                       verbose=True,compression=0)

#-----------------------------------------------------------------
# Setup boundary conditions
#-----------------------------------------------------------------

print 'Available boundary tags', domain.get_boundary_tags()
Bf = Field_boundary( path_fault+fault_filename, domain,\
                     time_thinning=1, mean_stage=tide,\
                     use_cache=True, verbose=True)
Bt = Transmissive_boundary(domain)

domain.set_boundary({'west': Bf,'south':Bf,'east': Bf,\
                                            'north': Bt})
domain.set_name(out_filename)
#-----------------------------------------------------------------
# Evolve system through time
#-----------------------------------------------------------------

import time
t0 = time.time()

from Numeric import allclose
from anuga.abstract_2d_finite_volumes.quantity import Quantity

# Save every 1 sec leading up to wave approaching land
for t in domain.evolve(yieldstep = resolucao_temporal,\
                                    finaltime=simulation_time):
```

```
    domain.write_time()
    domain.write_boundary_statistics(tags = ['west','south',\
                                                    'east'])


print 'That took %.2f seconds' %(time.time()-t0)
```